

DTIC FILE COPY

1

AD-A218 499

AN INTERACTIVE METHOD FOR ESTIMATING HAILSTONE SIZE  
AND CONVECTIVELY-DRIVEN WIND GUSTS FROM  
FORECAST SOUNDINGS

DTIC  
ELECTE  
FEB 23 1990  
S D D  
UC

John Philip Pino, B.S.

**DISTRIBUTION STATEMENT A**

Approved for public release:  
Distribution Unlimited

A Digest Presented to the Faculty of the Graduate  
School of Saint Louis University in Partial  
Fulfillment of the Requirements for the  
Degree of Master of Science (Research)

1989

90 02 21 058

**REPORT DOCUMENTATION PAGE**

Form Approved  
OMB No. 0704-0188

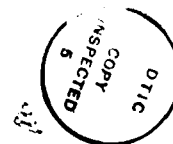
1a. REPORT SECURITY CLASSIFICATION <b>UNCLASSIFIED</b>		1b. RESTRICTIVE MARKINGS <b>NONE</b>	
2a. SECURITY CLASSIFICATION AUTHORITY		3. DISTRIBUTION / AVAILABILITY OF REPORT <b>APPROVED FOR PUBLIC RELEASE; DISTRIBUTION UNLIMITED.</b>	
2b. DECLASSIFICATION / DOWNGRADING SCHEDULE		4. PERFORMING ORGANIZATION REPORT NUMBER(S)	
4. PERFORMING ORGANIZATION REPORT NUMBER(S)		5. MONITORING ORGANIZATION REPORT NUMBER(S) <b>AFIT/CI/CIA- 89-048</b>	
6a. NAME OF PERFORMING ORGANIZATION <b>AFIT STUDENT AT SAINT LOUIS UNIVERSITY</b>	6b. OFFICE SYMBOL <i>(If applicable)</i>	7a. NAME OF MONITORING ORGANIZATION <b>AFIT/CIA</b>	
6c. ADDRESS (City, State, and ZIP Code)		7b. ADDRESS (City, State, and ZIP Code) <b>Wright-Patterson AFB OH 45433-6583</b>	
8a. NAME OF FUNDING / SPONSORING ORGANIZATION	8b. OFFICE SYMBOL <i>(If applicable)</i>	9. PROCUREMENT INSTRUMENT IDENTIFICATION NUMBER	
8c. ADDRESS (City, State, and ZIP Code)		10. SOURCE OF FUNDING NUMBERS	
		PROGRAM ELEMENT NO.	PROJECT NO.
		TASK NO.	WORK UNIT ACCESSION NO.
11. TITLE (Include Security Classification) <b>(UNCLASSIFIED)</b> <b>An Interactive Method for Estimating Hailstone Size and Convectively-Driven Wind Gusts From Forecast Soundings</b>			
12. PERSONAL AUTHOR(S) <b>John Philip Pino</b>			
13a. TYPE OF REPORT <b>THESIS/DISSERTATION</b>	13b. TIME COVERED FROM _____ TO _____	14. DATE OF REPORT (Year, Month, Day) <b>1989</b>	15. PAGE COUNT <b>98</b>
16. SUPPLEMENTARY NOTATION <b>APPROVED FOR PUBLIC RELEASE IAW AFR 190-1 ERNEST A. HAYGOOD, 1st Lt, USAF Executive Officer, Civilian Institution Programs</b>			
17. COSATI CODES		18. SUBJECT TERMS (Continue on reverse if necessary and identify by block number)	
FIELD	GROUP	SUB-GROUP	
19. ABSTRACT (Continue on reverse if necessary and identify by block number)			
20. DISTRIBUTION / AVAILABILITY OF ABSTRACT <input checked="" type="checkbox"/> UNCLASSIFIED/UNLIMITED <input type="checkbox"/> SAME AS RPT. <input type="checkbox"/> DTIC USERS		21. ABSTRACT SECURITY CLASSIFICATION <b>UNCLASSIFIED</b>	
22a. NAME OF RESPONSIBLE INDIVIDUAL <b>ERNEST A. HAYGOOD, 1st Lt, USAF</b>		22b. TELEPHONE (Include Area Code) <b>(513) 255-2259</b>	22c. OFFICE SYMBOL <b>AFIT/CI</b>

DIGEST

Interactive methods for forecasting potential hailstone size and convectively-driven surface wind gust velocities are applied to forecast soundings which better represent atmospheric conditions prior to the onset of convection. The forecast sounding is based upon the 1200 UTC sounding and is developed interactively by the user considering diurnal changes expected to occur in the lower tropospheric levels over the next 6-12 hours. Changes to the middle and upper levels are estimated by taking a fraction of the mean geostrophic advection of temperature for consecutive layers and adjusting the 1200 UTC sounding accordingly. Interactive capability allows for final adjustment of any or all of the data. Hailstone size and convectively-driven wind gusts are based upon key thermodynamic parameters (e.g., CCL, LFC, CAPE) derived from the forecast sounding. — AG 7-10-70

Hailstone size is determined using three separate routines. The first is based upon techniques described in AWS TR-200 which is a function of the CCL and is used extensively by the USAF Air Weather Service. The other two methods relate the hailstone size to its terminal velocity

<input checked="" type="checkbox"/>
<input type="checkbox"/>
<input type="checkbox"/>



Dist	Avail and/or Special
A-1	

odes

which in turn is a function of the maximum expected updraft in the cloud. For these methods, an algorithm considers the role of heat transfer from the environment to the hailstone during the stone's descent to account for melting.

Convectively-driven surface wind gusts are estimated three ways. One method automates a technique described in AWS TR-200. In the second method, the wind gust is a function of the temperature of a parcel brought down from the Level of Free Sink (LFS) moist-adiabatically to the surface and the surface environmental temperature. A third method integrates Anthes' vertical motion equation downward from the LFS to the surface.

Hail and strong wind proximity soundings from AVE-SESAME I and II and OK PRE-STORM were used to validate the procedures. For 58 cases studied, the Pino-Moore hail method resulted in a Student-t statistic significant at the 0.5% level compared with a 10% level for the AWS TR-200 technique. The forecast sounding algorithm produced a mean diameter error of +0.03 cm compared to -1.18 cm for 15 proximity soundings. Validation of the three wind gust methods resulted in little discriminatory skill but the bias and scatter scores did favor Anthes method as more operationally suitable.

AN INTERACTIVE METHOD FOR ESTIMATING HAILSTONE SIZE  
AND CONVECTIVELY-DRIVEN WIND GUSTS FROM  
FORECAST SOUNDINGS

John Philip Pino, B.S.

A Thesis Presented to the Faculty of the Graduate  
School of Saint Louis University in Partial  
Fulfillment of the Requirements for the  
Degree of Master of Science (Research)

1989

COMMITTEE IN CHARGE OF CANDIDACY

Associate Professor James T. Moore,  
Chairperson and Advisor

Professor Yeong-Jer Lin

Professor Gandikota V. Rao

## ACKNOWLEDGEMENTS

My deepest appreciation is extended to Dr James Moore for his guidance and technical support throughout my research. I would also like to offer gratitude to Professors Rao and Lin for their expert advice. Also, the Air Weather Service of the United States Air Force for offering me the opportunity to attend graduate school.

I cannot complete my acknowledgements without mentioning the spiritual support and understanding I received from my wife, Elaine. Her patience and encouragement on countless occasions enabled me to complete this degree.

## TABLE OF CONTENTS

Chapter 1. Introduction to the Problem .....	1
Chapter 2. Review of Related Literature ....	5
2.1 Forecasting Hailstone Size.....	5
2.2 Estimating Convectively-Driven Wind Gusts .....	14
2.3 The Forecast Sounding .....	16
Chapter 3. The Procedure .....	18
3.1 Hail Size Formulation .....	18
3.1.1 Calculating the Vertical Updraft .....	18
3.1.2 Drag Coefficient and Hailstone Density .....	23
3.1.3 Hailstone Melting .....	24
3.2 Estimating Convective Wind Gusts ..	30
3.3 The Forecast Sounding Algorithm ...	31
3.3.1 Diurnal Changes .....	31
3.3.2 Middle and Upper Level Changes .....	35
3.4 Validation Procedures .....	36
3.5 The Sounding Analysis Package .....	40
Chapter 4. Results and Discussion .....	42
4.1 Hail Size Forecast Validation .....	44
4.1.1 Combined Cases .....	44
4.1.2 Composite Soundings .....	50
4.2 Convective Wind Gust Validation ...	56
4.3 Sensitivity Study of Key Variables	60
4.4 Forecast Sounding Utility .....	62

4.4.1	Limitations and Weaknesses .	66
4.5	Case Study .....	68
Chapter 5.	Summary and Conclusions .....	83
5.1	Research Summary .....	83
5.2	Future Considerations .....	86
APPENDIX	.....	88
REFERENCES	.....	95
BIOGRAPHY OF THE AUTHOR	.....	98

## LIST OF TABLES

Table		Page
1	Modifying factors for Planetary Boundary Layer interactively accounted for in the forecast sounding algorithm. ....	32
2	Conversion table of descriptive hail sizes to actual measured diameters. ....	38
3	Parameters calculated by the Pino-Moore sounding analysis algorithm. ....	41
4	Example of the Pino-Moore sounding analysis. Note: for hail sizes, estimates in parentheses are values prior to melting. ..	
5	Results of the composite sounding hail size estimates as computed by Pino-Moore and Fawbush-Miller techniques. ....	54
6	Results of the sensitivity study for the hailstone drag coefficient, density, and the level of hail formation. Numbers in parentheses indicate error. ....	54
7	Validation results for the forecast sounding algorithm. Numbers in parentheses indicate error. ....	65
8	Sounding analysis for the 1200 UTC 20 February 1989 Jackson, MS sounding. ....	71
9	Sounding analysis for the 0000 UTC 21 February 1989 Jackson, MS forecast sounding (diurnal changes only). ....	75
10	Same as Table 9 except diurnal changes plus geostrophic thermal advection. ....	76
11	Sounding analysis for the 0000 UTC 21 February 1989 Jackson, MS sounding. ....	81

## LIST OF FIGURES

Figure		Page
1	Positive area approximated by Fawbush-Miller technique. BB' is the base of the positive triangle and HH' measures the altitude. ....	6
2	The Fawbush-Miller Hail Graph showing the forecast hailstone diameter in inches. ....	7
3	Correction nomogram for Fambush-Miller hail technique. ....	8
4	Comparison of updraft velocity estimated from balloon ascent rate (solid line) and from parcel buoyancy (dashed line). Height in kilometers MSL. ....	13
5	Example sounding with corresponding positive and negative areas as computed from the LFC and CCL. Dashed lines slanting to the left are dry adiabats, dashed lines slanting to the right are constant mixing ratio lines, dashed-dot lines are moist adiabats. ....	
6	Idealized energy input by surface heating (shaded area is one energy box). Total heat realized is 50 boxes ( $350 \text{ J kg}^{-1}$ ); $\Delta t$ is time from sunrise. E is energy realized for a given $\Delta t$ (in boxes). ....	34
7	Scatter diagram with statistical analysis for Pino-Moore hail diameter estimates versus observed hail diameters. ....	45
8	Scatter diagram with statistical analysis for Fawbush-Miller hail diameter estimates versus observed hail diameters. ....	46
9	Scatter diagram with statistical analysis for Fawbush-Miller hail diameter estimates without melting. ....	49
10	Mean temperature and dewpoint temperature for air masses producing hailstones 1/2 inch in diameter, 68 cases. ....	51
11	Mean temperature and dewpoint temperature for air masses producing hailstones 1 inch in diameter, 25 cases. ....	52

12	Mean temperature and dewpoint temperature for air masses producing hailstones 4 inches in diameter, 2 cases. ....	53
13	Scatter diagram with statistical analysis for winds estimated by Foster method versus observed wind gusts. ....	57
14	Scatter diagram with statistical analysis for winds estimated by Fawbush-Miller method versus observed wind gusts. ....	58
15	Scatter diagram with statistical analysis for winds estimated by Anthes method versus observed wind gusts. ....	59
16	Upper air sounding for Jackson, MS at 1200 UTC 20 February 1989. ....	70
17	Forecast sounding (diurnal changes only) for Jackson, MS at 0000 UTC 21 February 1989. ....	72
18	Forecast sounding (diurnal changes and geostrophic thermal advection) for Jackson, MS at 0000 UTC 21 February 1989. ....	73
19	Surface temperatures and dewpoint temperatures for Louisiana and Mississippi stations at 2100 UTC 20 February 1989. ....	79
20	Upper air sounding for Jackson, MS at 0000 UTC 21 February 1989. ....	80

## 1. INTRODUCTION TO THE PROBLEM

During the early 1950's, the Air Weather Service (AWS) of the United States Air Force undertook a major study dealing with severe thunderstorm forecasting. The study was headed by Lt. Col. Ernest Fawbush and Maj. Robert Miller with the primary goal of improving AWS's capability for providing severe thunderstorm support to varied customers within the Department of Defense (DoD) along with its numerous missions. The result of this study, "Notes On Analysis and Severe-Storm Forecasting Procedures of the Air Force Global Weather Central" (AWS Technical Report 200, 1972), provides techniques for hand calculating potential hailstone size and convectively-driven surface wind gust velocities. For the past 35 years, AWS has issued countless warnings for severe thunderstorms, many of which included specific user-oriented information for hailstone size and convectively-driven surface wind gust velocities derived from the procedures described in AWS TR-200.

As the physical and dynamical understanding of thunderstorms and their environment evolved during the past twenty five years, AWS recognized the

need and, more importantly, the capability for improved customer support by considering the temporal changes of the atmosphere between rawinsonde sampling times (12 UTC and 00 UTC). Gesser and Wallace (1986) describe a technique for forecasting changes for an air mass from its sampling time at 12 UTC to the estimated time of convective development, usually some 6 to 12 hours later.

The Air Weather Service is about to undergo a complete revolution in its customer support during the early 1990's with the acquisition of the Automated Weather Distribution System (AWDS) and the Next Generation Weather Radar (NEXRAD). These major programs possess the capability of automating many of the day-to-day "routine" tasks forecasters perform. Consequently, many forecasting techniques, such as those in AWS TR-200, can now be automated.

Although automating the AWS TR-200 techniques for forecasting hail size and wind gust velocities is a logical first step, AWS can now work towards improving its severe storm support. An advanced system such as AWDS provides AWS with the capability of incorporating more sophisticated techniques into

its diagnosis and short-term forecasts of the severe storm environment. A critical part of determining the atmosphere's potential for severe convection is the comprehensive diagnosis of the pre-storm sounding. Additionally, there is a definite need to develop an automated forecast sounding technique which would permit interaction with the forecaster on a "what-if" basis, allowing him to create a likely thermodynamic profile for 6-12 hours from 1200 UTC. These two steps alone would enhance the AWS's severe thunderstorm forecasting capability by exploiting the knowledge gained in this area over the past 2-3 decades.

The major thrust of this research is to develop viable, automated methods for forecasting potential hailstone size and surface wind gusts from rawinsonde data. These methods will be applied to objectively-derived forecast soundings which better represent atmospheric conditions prior to the development of convection. Diagnostic methods will be developed, based upon recent developments in understanding severe convection, which offer a more complete diagnosis of the morning sounding. Techniques to produce a 6-12 h forecast sounding will be discussed and tested on special case studies

to evaluate their utility in the operational environment. Forecast schemes for hail size and convective wind gust determination will be described which more fully exploit the thermodynamic profile at a station. The ultimate goal is to develop operationally useful diagnostic/prognostic tools which would improve the forecasting of severe weather attending strong convection.

## 2. REVIEW OF RELATED LITERATURE

### 2.1 FORECASTING HAILSTONE SIZE

The Air Weather Service forecasting techniques for hail size and maximum wind gusts of convective origin are described in Chapters 9 and 10, respectively, of the AWS Technical Report 200. The technique for forecasting hail size requires the use of a nomogram (Fig. 1). Tracing the moist adiabat from the CCL to the pressure level where the dry-bulb air temperature is  $-5^{\circ}\text{C}$  forms the first side of a triangle defining the positive area. This pressure level, the dry-bulb temperature curve, and the moist adiabat through the CCL form the triangle representing the positive area. After determining the base (horizontal coordinate) and altitude (vertical coordinate) of the positive triangle, a hailstone diameter of up to four inches can be interpolated from a nomogram (Fig. 2).

A correction (reduction) based on the height of the Wet-Bulb-Zero (WBZ) can then be made using the nomogram shown in Fig. 3. This nomogram requires the height of the  $0^{\circ}$  wet bulb isotherm (vertical coordinate) and the hail size previously determined (horizontal coordinate) from Fig. 2. This

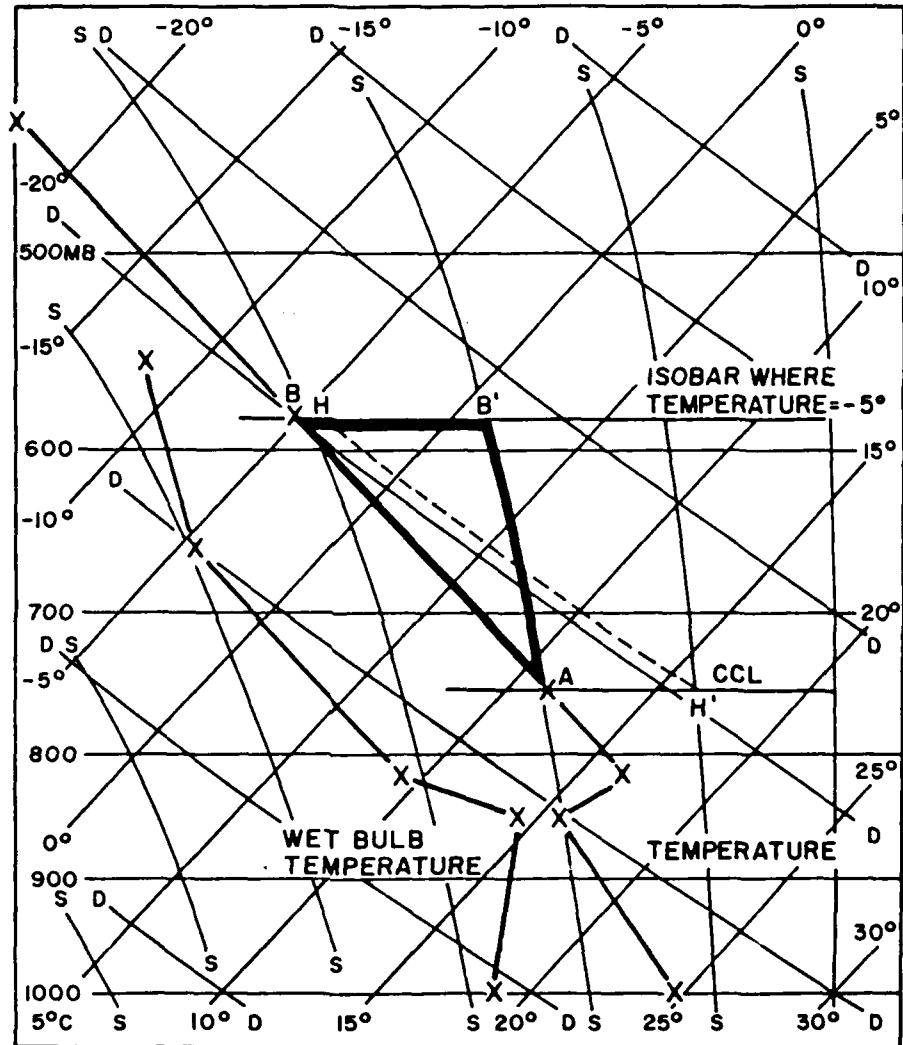


Fig. 1 Positive area approximated by Fawbush-Miller technique. BB' is the base of the positive triangle and HH' measures the altitude. (AWS TR-200)

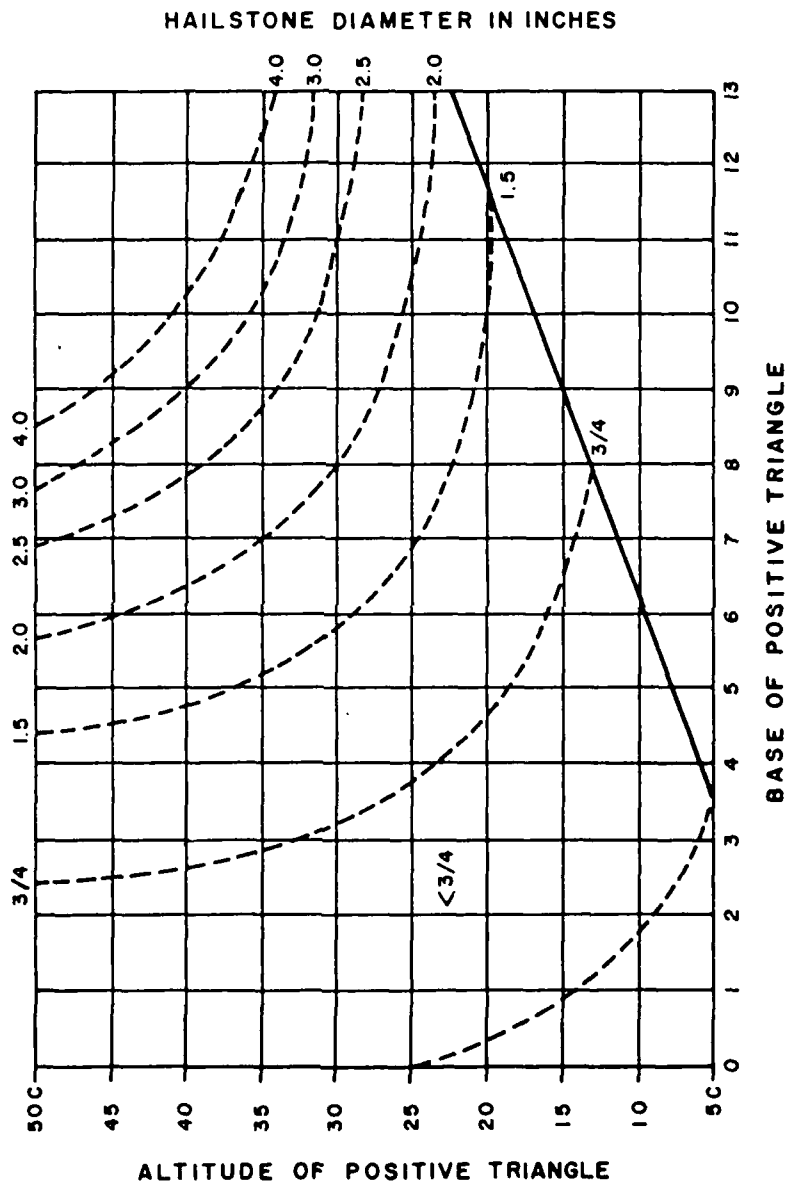


Fig. 2 The Fawbush-Miller Hail Graph showing the forecast hailstone diameter in inches. (AWS TR-200)

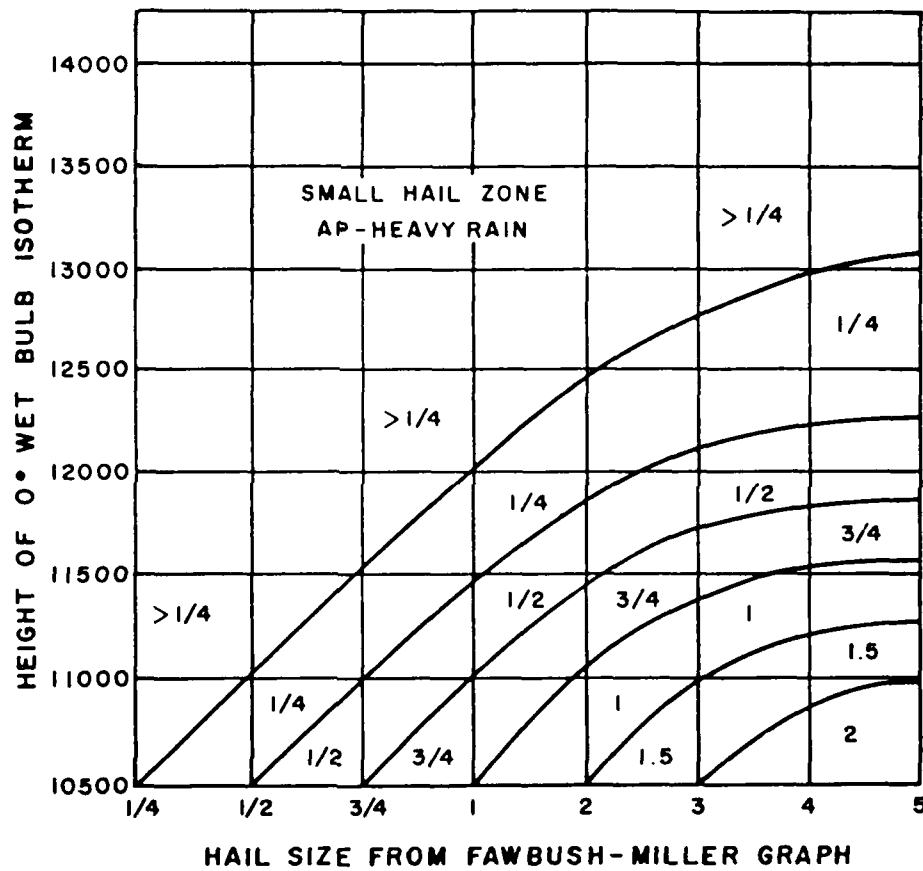


Fig. 3 Correction nomogram for Fambush-Miller hail technique. (AWS TR-200)

correction is made only for cases where the WBZ height is above 10,500 feet.

Bilham and Relf (1937) considered a spherical hailstone of diameter,  $d$ . When dropped from rest in a quiescent atmosphere, the hailstone will accelerate downward until the aerodynamic drag force is just equal to the hailstone weight thus reaching its terminal velocity.

$$C_d \rho_a V_h^2 \pi \frac{d^2}{4} = \rho_h g \pi \frac{d^3}{6} \quad (1)$$

The left-hand side of (1) is the expression for the drag of the hailstone where  $C_d$  is the drag coefficient,  $\rho_a$  is the density of air computed using the equation of state at the pressure level of hail formation, and  $V_h$  is the terminal velocity of the hailstone. The right hand-side is equal to the hailstone's weight where  $\rho_h$  is the density of ice,  $g$  is the acceleration of gravity, and  $d$  is the diameter of the hailstone.

Solving (1) for  $V_h$  yields:

$$V_h^2 = \frac{2 \rho_h g d}{3 \rho_a C_d} \quad (2)$$

In (2)  $V_h$  can be thought of as the downward velocity required to make the viscous force equal to the gravitational force in (1); i.e., no acceleration takes place. Foster and Bates (1956) assumed that the environmental upward vertical velocity required to suspend the hailstone is nearly equal to this terminal velocity. The updraft within the thunderstorm provides this necessary suspension. Their technique for relating the suspending updraft to hailstone diameter is based on the following premises:

1. the updraft velocity prevailing in the zone of hail formation is the velocity required to just sustain the fully grown hailstone (i.e., the stone's terminal velocity),

2. this updraft velocity is derived from the buoyancy force acting on parcels in the updraft above the level of free convection (LFC),

3. this velocity (and, therefore, the hail size) may be calculated from the positive area below the level of hail formation as determined on a thermodynamic diagram of a sounding of the air mass taken very close to the site and time of the hail occurrence.

Foster and Bates (1956) relate the vertical accelerations of a non-entraining parcel to the buoyancy force given by

$$\dot{w} = g \left( \frac{T' - T}{T} \right) \quad (3)$$

where  $\dot{w}$  is the vertical acceleration of a parcel,  $T'$  is the temperature of the parcel, and  $T$  is the temperature of the environment. Upon integration,

$$w_h = \frac{g}{T_m} (\Delta T_H H)^{\frac{1}{2}} \quad (4)$$

where  $w_h$  is the vertical velocity at the height of hail formation,  $T_m$  is the mean temperature of the environment from the LFC through height  $H$ , the level of hail formation,  $\Delta T_H$  is the difference of the parcel temperature and the environmental temperature at the level where the parcel temperature is  $-10^\circ\text{C}$  and  $w$  at the LFC is assumed to be zero. The diameter of a potential hailstone can now be calculated by substituting  $w_h$  for  $V_h$  in (1) yielding:

$$d = \frac{3 \rho_a c_d w_h^2}{2 \rho_h g} \quad (5)$$

Bluestein et al. (1988) analyzed soundings

obtained by a storm-intercept crew using mobile sounding units. A sounding was launched into the wall cloud of a severe storm near Canadian, Texas on 7 May 1986. Neglecting the effects of water loading and vertical perturbation pressure gradients, a vertical updraft speed profile was calculated and compared with the measured updraft speeds (Fig. 4). In the calculated updraft profile, the vertical velocity above the LFC at height  $h$  is a function of the convective available potential energy (CAPE). Bluestein assumed that the parcel's vertical velocity is near zero at the LFC. Both profiles are in close agreement between 2.3 and 7.2 km, thus validating the parcel method of estimating vertical velocities.

Based on the techniques described by Prosser and Foster (1966), an effort was undertaken by the National Severe Storms Forecast Center (NSSFC) to determine the utility of calculating potential hailstone size and wind gust velocities from operational rawinsonde data. Since the hail algorithm rarely calculated hail potentials greater than one inch and the wind algorithm resulted in little discriminatory skill, the authors concluded that these algorithms be dropped from the NSSFC

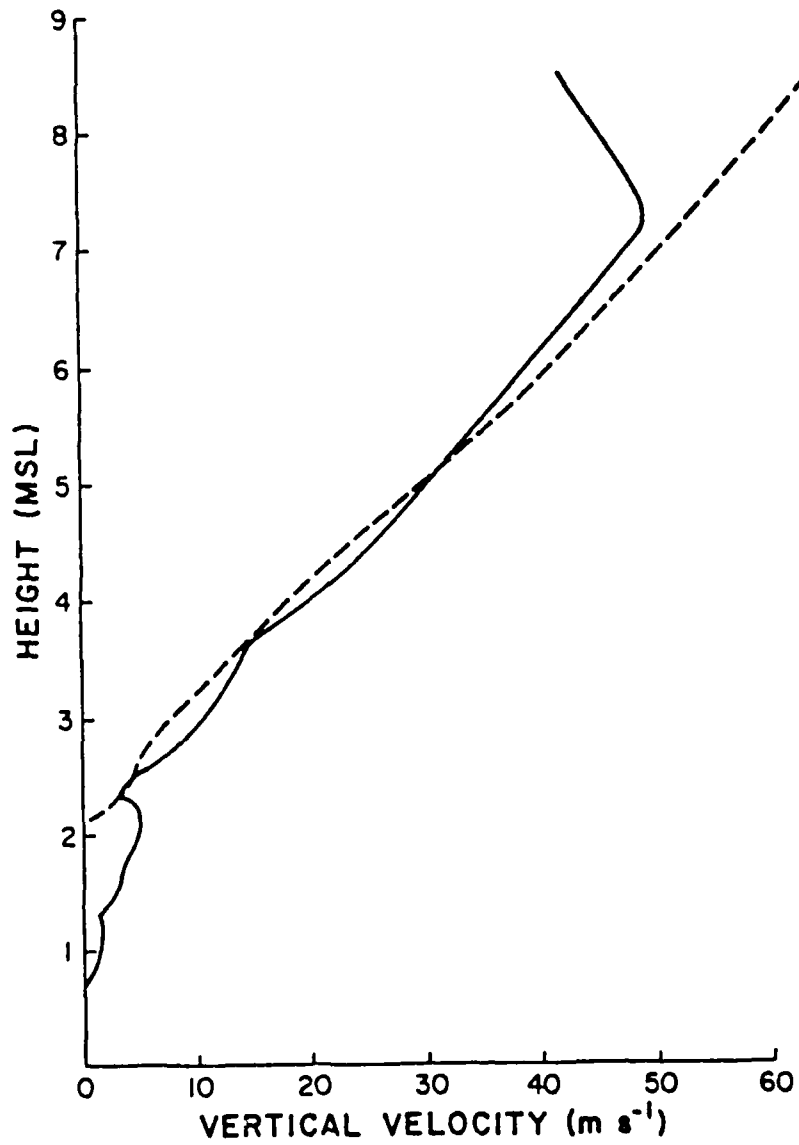


Fig. 4 Comparison of updraft velocity estimated from balloon ascent rate (solid line) and from parcel buoyancy (dashed line). Height in kilometers MSL. (Bluestein et. al. 1988)

computerized raob analysis package.

Leftwich (1984) applied Foster and Bates' technique to assess the predictive potential of rawinsonde data close in time and space to hail events. Leftwich considered 12 hail events which occurred within 100 km and  $\pm 2$  h of a rawinsonde sounding. Leftwich (1986) continued this investigation obtaining hail size estimates based on VISSR Atmospheric Sounder (VAS) data for 5 hail events. He concluded that when using representative airmass soundings, his one-dimensional model produced encouraging results which favored continued efforts in developing an operational objective aid for the Severe Local Storm (SELS) forecast unit forecaster.

## 2.2 ESTIMATING CONVECTIVELY-DRIVEN WIND GUSTS

Fawbush and Miller (1954) present a procedure for forecasting peak wind gusts in non-frontal thunderstorms. This technique is still used today by the Air Weather Service. Their study revealed a relationship between peak wind gusts and the temperature difference between the surface air underneath and in advance of the thunderstorm. The

"downrush" temperature under the thunderstorm is forecast by lowering the wet-bulb freezing level temperature to the surface along a saturation adiabat. The difference between the surface temperature and the downrush temperature,  $t$ , is used to compute a peak gust according to (6):

$$\text{Peak Gust} = 7 + 3.06t - 0.0073t^2 - 0.000284t^3 \quad (6)$$

Foster (1958) integrates the bouyancy equation to find the downward speed of a parcel of air that becomes cooler than its environment and sinks to the ground. He approximates the downrush speed according to:

$$w_o = - \left( - \frac{g Z \Delta T_o}{T_m} \right)^{\frac{1}{2}} \quad (7)$$

where  $w_o$  is the vertical velocity of the parcel at the surface,  $Z$  is the height above ground of the level where the descending parcel and the environment have equal temperatures (the level of free sinking),  $\Delta T_o$  is the difference at the surface of the environment temperature and the "mid-way moist adiabat", and  $T_m$  is the mean temperature of the parcel in descent.

Foster (1958) as well as Fawbush and Miller (1954) point out that surface gusts may be influenced by the speed of the thunderstorm. To test this possible effect, Foster averaged the winds at 700 and 500 mb for each of the 100 cases and the resulting speed was added to the computed downdraft speed. However, this yielded a correlation coefficient of 0.51, an improvement of only 0.01 compared to the results without this correction.

### 2.3 THE FORECAST SOUNDING

Doswell et al. (1982) first conclusion confirmed the premise that to determine more accurate hailstone size and wind gust velocities, a more representative profile of the atmospheric conditions prior to the onset of convection is necessary. Gesser and Wallace (1985) offer a useful but subjective approach in which adjustments to the 12 UTC sounding are determined primarily by estimating thermal advection at 850, 700, and 500 mb using standard upper air analyses. Crum and Cahir (1983) considered using subjective methods along with numerical guidance to estimate changes in the environmental profile. The modifications included upper air changes, vertical exchange simulations,

and surface dewpoint changes. These changes were tested for the subsequent impact in real-time forecasts of shower-top elevation calculated by the Anthes (1977) 1-d cloud model. Their results indicated that modification of the sounding, particularly in the lower levels, produced better forecast estimates of the shower cloud tops. In particular, knowledge of the afternoon surface dewpoints prior to convective development produced estimates of shower-top elevations better than or equal to any other modification.

McGinley (1986) offers a method for estimating the diurnal changes for the lowest 1.5 km of a sounding by considering explicitly the sensible warming from the ground. This heating process can be prominent for dynamically weak situations. This method is addressed in section 3.3.1.

### 3. THE PROCEDURE

#### 3.1 HAIL SIZE FORMULATION

##### 3.1.1 CALCULATING THE VERTICAL UPDRAFT

Foster and Bates' technique only considers a non-entraining buoyancy force in determining the vertical velocities. A proposed methodology adapts their technique but employs the vertical velocity equation from the Anthes (1977) one-dimensional cloud model,

$$\frac{d\left(\frac{w^2}{2}\right)}{dz} = g \frac{B}{(1+\alpha)} - g Q_{tw} - \mu w^2 \quad (8)$$

where  $w$  is the vertical velocity,  $g$  is gravity,  $\mu$  is the entrainment rate given by  $0.183/R$  where  $R$  is the radius of the cell (2000 m),  $\alpha$  is the "virtual mass coefficient" equal to 0.5 which compensates for the neglect of nonhydrostatic pressure perturbations, and  $Q_{tw}$  is the total liquid water content expressed as the ratio of the mass of water to the mass of air. The buoyancy term  $B$  is given by

$$B = \frac{(T_{vc} - T_{ve})}{T_{ve}} \quad (9)$$

where  $T_{vc}$  and  $T_{ve}$  are the virtual temperature of the cloud updraft and the environment, respectively.

The virtual temperature of the cloud updraft is determined by

$$T_c = \frac{T'_c + (\exp(\mu\Delta z) - 1)T_{ve}}{\exp(\mu\Delta z)} \quad (10)$$

where  $T'_c$  is the cloud temperature before mixing with the environmental air and  $z$  is the change of height between computational levels. The retarding effects on the parcel's acceleration due to liquid water drag and entrainment of slow-moving air from outside the upward-moving parcel are included in the second and third right-hand side (RHS) terms of (8).

Upon integration, in a pressure coordinate form, (8) becomes

$$w_u^2 = w_l^2 + 2R_d \left( \frac{(T_{vc} - T_{ve})}{(1 + \alpha)} - T_{ve}Q_{tw} - \frac{T_{ve}}{g} \mu w^2 \right) \ln \frac{P_l}{P_u} \quad (11)$$

In the proposed model,  $w_u$  is calculated using a boot strap method in increments less than or equal to 15 mb from both the LFC and the Convective Condensation Level (CCL) up to the level of hail formation. Foster and Bates (1956) determined that the representative level of hail formation is where the parcel temperature is equal to  $-10^\circ\text{C}$ . Estimates of the potential hailstone size can then be

calculated by substituting the  $w_u$ 's based upon the positive areas above the LFC and CCL into (5).

Figure 5 depicts the positive and negative areas defined by the CCL and LFC. The proposed algorithm first determines the lifting condensation level (LCL) by computing the average potential temperature and the average mixing ratio of the lowest 100 mb of the sounding. This is done by calculating the potential temperature over a small layer and multiplying that temperature by the fraction that that layer is of 100 mb. Whereas the average potential temperature is computed by a pressure weighting scheme, the average mixing ratio is weighted according to  $p^k$ .

Further lifting of the parcel along a moist adiabat causes the parcel to reach its LFC. Areas 2 and 3 represent the negative areas proportional to energy. A mechanical lifting process such as frontal and orographic lifting, or convergence is required to overcome this negative area in order for the parcel to reach its LFC. Upon reaching the LFC, the parcel becomes warmer than the surrounding environment resulting in the positive area labeled 1 bounded by the moist adiabat and the dry-bulb

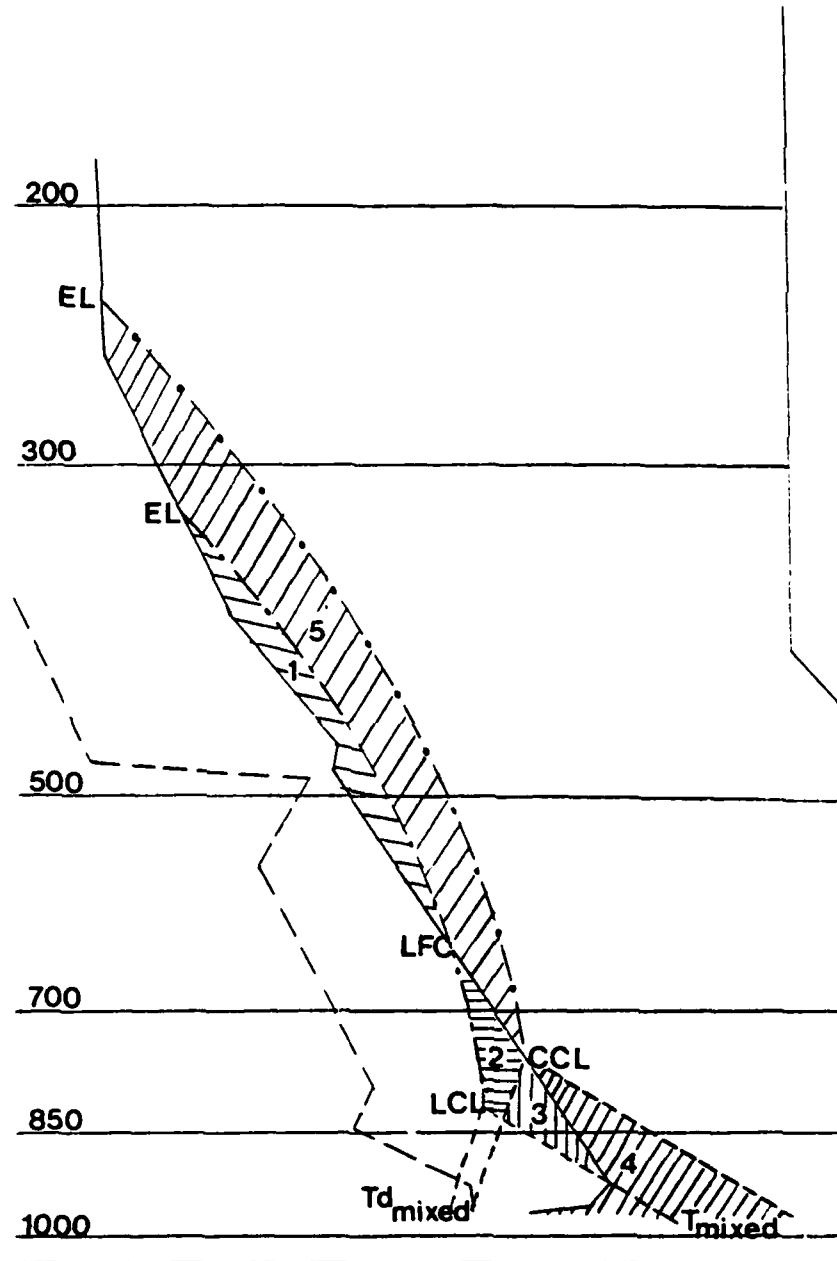


Fig. 5 Example sounding with corresponding positive and negative areas as computed from the LFC and CCL. Dashed lines slanting to the left are dry adiabats, dashed lines slanting to the right are constant mixing ratio lines, dashed-dot lines are moist adiabats.

temperature curve. This positive area is proportional to the amount of kinetic energy gained by the parcel from the environment. The positive area bounded by the pressure level where the parcel temperature is  $-10^{\circ}\text{C}$ , the dry-bulb curve, and the moist adiabat represents the energy which is used in computing the vertical updraft.

In situations where a lifting mechanism is not available to overcome the negative area, diurnal heating may supply the necessary energy for convection to develop. The algorithm determines the intersection of the dry-bulb curve and the mixing ratio corresponding to the surface dewpoint temperature. This intersection defines the parcel's CCL. Tracing this CCL along a dry adiabat down to the surface pressure level determines the convective temperature. Area 4 is the energy needed by diurnal heating for the parcel to reach its convective temperature. Lifting the parcel moist adiabatically from the CCL until the dry-bulb curve is intersected again defines the other EL based on the CCL. The positive areas labeled as 1 and 5 are used by the algorithm to calculate the vertical updraft.

In an operational setting, the forecaster must

decide what type of triggering mechanism will initiate the expected convection. As seen in Fig. 5, the amount of energy available is quite different depending upon what type of trigger is anticipated. It is for this reason that the forecaster needs to be aware of what mechanisms or physical processes will initiate the convection. If convection due to diurnal heating is expected, the forecaster would base his estimate of hailstone size as predicted by the updraft formed from the energy from areas 1 and 5, i.e., the CCL approach. If a lifting mechanism is expected, the forecaster could adjust the hail size estimate to correspond with the updraft formed from area 1, i.e., the LFC approach.

### 3.1.2 DRAG COEFFICIENT AND HAILSTONE DENSITY

Macklin and Ludlam (1961) concluded from their experiments that a reasonable mean value of the drag coefficient for large, asymmetrical hailstones greater than 1 cm in diameter is 0.6. Prosser and Foster (1966) also incorporated a drag coefficient of 0.6 in their technique. This value is considerably lower, 45% lower, than the mean value of 0.87 given by Matson and Huggins (1980). Matson and Huggins' value is based on velocity data

obtained for about 600 relatively small hailstones in the diameter range of 5-25 mm. The hailstones were sampled in southeast Wyoming, southwest Nebraska and northeast Colorado. For this investigation, however, a drag coefficient of 0.6 was adopted since it best represents the relative sizes and shapes of those stones which are being estimated. In section 4.0 tests will be shown demonstrating the sensitivity of our calculations to the assumed drag coefficient.

Mason (1953) considered solid ice spheres having densities of  $0.92 \text{ g cm}^{-3}$ . Since hailstones are rarely solid ice but often composed of ice with embedded air pockets (Knight and Knight, 1970), this research used a density value of  $0.90 \text{ g cm}^{-3}$ . Macklin (1963) and Prosser and Foster (1966) also used this value in their studies while Matson and Huggins (1980) chose a value of  $0.89 \text{ g cm}^{-3}$ .

### 3.1.3 HAILSTONE MELTING

Fawbush and Miller (1953) concluded, from their analyses of 274 soundings, that the size of hailstones will generally be the same at the surface and aloft when the wet-bulb freezing level is less

than 11000 feet above the surface and that hailstones maintain their size for at least 9000 feet of free fall, after which rapid melting and disintegration take place. Their report further correlated this melting to the observed WBZ height. As the WBZ height increases, the number of large hailstones reported decreased rapidly compared to those for the 7000-9000 foot range.

These conclusions prompted further research into the melting rate of hailstones. Mason (1956) calculated the rate of melting of solid ice spheres (less than 3 mm in radius) and of graupel particles as they fall from the  $0^{\circ}\text{C}$  level towards the ground. Assuming the overall radius of the particle at any moment is  $b$  and the radius of the unmelted core is  $a$ , the thickness of the water film is simply  $(b-a)$ . As the hailstone falls through clear air, heat is gained from the surrounding environment mainly by conduction and convection. Additionally, if its surface temperature is below the dew point of the environment, the hailstone will gain heat by condensation of water vapor upon its surface. If the air is dry, the hailstone may lose heat by evaporation. The basic equations representing the transfer of heat between the environment and the

hailstone are

$$L_f 4 \pi a^2 \rho_i \frac{da}{dt} = -4 \pi a b K_w T_s / (b-a) =$$

(latent heat of melting) (transfer through water)

$$- \left( 4 \pi b K_a C (T_a - T_s) + L_v 4 \pi b D C (\rho_v - \rho_v(s)) \right)$$

(conduction through air) (condensation on surface)

(12)

In (12),  $T_s$  is the surface temperature of the hailstone and  $T_a$  is the temperature of the environment;  $L_f$ ,  $L_v$  are the latent heats of fusion and evaporation,  $K_w$ ,  $K_a$  the thermal conductivities of water and air,  $D$  the diffusion coefficient of water vapor in air,  $\rho_i$  the density of the hailstone,  $C = 1.6 + 0.3(\text{Re})^{1/2}$ , a ventilation coefficient which takes into account the increased rate of heat flow towards a falling sphere of Reynolds number  $\text{Re}$ , and  $\rho$ ,  $\rho(s)$  are, respectively, the water-vapor concentrations in the remote environment and in the immediate vicinity of the surface of the particle.

Assuming the atmosphere is saturated, the saturation vapor densities appropriate to the temperatures  $T_a$  and  $T_s$  may be substituted for the values of  $\rho$  and  $\rho(s)$ . We further assume that over a small range of temperatures, say  $10^\circ\text{C}$ , the saturation vapor density may be regarded as a linear function of temperature, i.e.,

$$\rho_s(T_a) - \rho_s(T_s) = \beta(T_a - T_s) \quad (13)$$

where  $\beta$  is constant.

Equation (12) can now be rewritten as

$$\frac{da}{dt} = - \frac{\frac{K_w T_s}{L_f \rho_i} \frac{b}{a}}{(b-a)} \quad (14)$$

where

$$T_s = \frac{T_a}{\left(1 + \frac{K_w}{C(K_a + L_v D \beta)} \frac{a}{(b-a)}\right)} \quad (15)$$

In this particular investigation, the thickness of the water film was set at 1 mm.

Melting rates were obtained from Mason's method by integrating (14) downward with respect to time from the level of hail formation to the surface. The algorithm calculates the height between levels (less than or equal to 15 mb) the hailstone falls and determines the time the stone was subjected to the mean temperature of the layer given the stone's terminal velocity. Since this study is interested in calculating maximum potential hail stone sizes, it is assumed that the hailstones fall within the

"protective" downdraft of the thunderstorm. For this reason, the temperature of the downdraft at any height  $z$  is computed using the method presented by Foster (1958).

Macklin (1963) also examined heat transfer from spherical hailstones in addition to oblate spheroids. His experiments determined the dependence of the rate of heat transfer on shape by measuring the rate of melting of spheres and spheroids of ice in an airstream. While Mason's study dealt with stones having radii of 3 mm, Macklin's research included larger stones. For large hailstones, the water film is so thin that the surface temperature may be taken to be  $0^{\circ}\text{C}$ . Macklin cites that "it has been shown that the rate of removal of water from the stagnation point of a blunt-nosed ice object melting in an airstream is sufficiently rapid for the effect of the water film to be neglected."

Macklin represents the rate of melting of a spheroidal hailstone falling in clear air with its shortest axis vertical as

$$\frac{dm}{dt} = \frac{\chi A \text{Re}^{\frac{1}{2}} \beta}{2aL_f} \quad (16)$$

Since  $m = \frac{4}{3}\pi\delta a^3\alpha$ , then for constant  $\alpha$

$$\frac{da}{dt} = \frac{\chi\gamma Re^{\frac{1}{2}}\beta}{2\alpha\delta L_f} \left(\frac{1}{a}\right) \quad (17)$$

where  $m$  is the mass of the hailstone,  $\alpha$  is the ratio of minor to major axes of a spheroid or 1.0 for spheres,  $\chi$  is the numerical factor in the heat transfer coefficient experimentally found to be 0.76 when  $\alpha$  is 1.0,  $Re$  the Reynold's number,  $a$  the radius of the sphere,  $A$  the surface area of the sphere,  $\gamma$  the ratio of the surface area of a spheroid to that of a sphere of the same diameter (1.0), and  $\delta$  the density of the hailstone.

In (17), beta is defined as

$$\beta = Pr^{\frac{1}{3}}k\Delta T + Sc^{\frac{1}{3}}L_v D\Delta\sigma \quad (18)$$

where  $Pr$  is the Prandtl number,  $k$  the thermal conductivity of air,  $\Delta T$  the difference in temperature between the hailstone surface and the environment or downdraft,  $Sc$  the Schmidt number,  $L_v$  the latent heat of vaporization of water,  $D$  the coefficient of molecular diffusion of water vapor in air,  $\Delta\sigma$  the difference in water-vapor density

between the hailstone surface and the environment. Macklin experimentally found the Prandtl and Schmidt numbers to be 0.71 and 0.60 respectively. To determine  $\Delta\sigma$ , Mason's assumption represented as (13) was adopted.

To calculate Macklin's rate of melting, (17) is integrated downward from the level of hail formation similar to the algorithm after Mason. Since (13) is needed to compute beta, a value for  $T_s$  is represented as (15).

Preliminary test cases indicated Mason and Macklin's melting rates to be comparable. Since Macklin included large hailstones into his study, it was decided to incorporate this algorithm into the model.

### 3.2 ESTIMATING CONVECTIVE WIND GUSTS

Algorithms were developed after the Fawbush-Miller (1954) and Foster (1958) methods described in section 2. A third scheme adapting Foster's ideas was also included. While Foster's method accounted for a non-entraining buoyancy force, the third technique integrates Anthes' vertical velocity

equation from the LFS downward.

### 3.3 THE FORECAST SOUNDING ALGORITHM

#### 3.3.1 DIURNAL CHANGES

In light of Crum and Cahir (1983), the methodology for an automated forecast sounding first considers diurnal changes in the planetary boundary layer. An algorithm based on McGinley (1986) and Sellers (1965) computes the estimated surface heating as a function of the day of the year and the hours of sunlight. The daily total solar radiation incident at the top of the atmosphere can be determined by

$$Q_s = \frac{1440}{\pi} S \left( \frac{d}{d} \right)^2 (H \sin\phi \sin\delta + \cos\phi \cos\delta \sin H) \text{ lyday}^{-1} \quad (19)$$

Like McGinley, the algorithm allows 18% of the incident energy for sensible heating of the boundary layer. Modifying factors given in Table 1 are interactively accounted for in the algorithm.

The cumulative number of "boxes" on a Skew-T diagram by hour can be estimated by

CLOUD COVER:	
OVERCAST	0.5
BROKEN	0.7
SCATTERED	0.9
HAZE OR MOIST AIR	0.8
SURFACE MOISTURE/WATER	0.7
ICE/SNOW COVER	0.2
COMBINATIONS:	
ICE/SNOW, OVERCAST	0.1
SURFACE MOISTURE, HAZE, SCT	0.6

Table 1 Modifying factors for the Planetary Boundary Layer interactively accounted for in the forecast sounding algorithm. (McGinley 1986)

$$E(t) = E_t \frac{\left(1 - \cos\pi\left(\frac{t-t_r}{T_s}\right)\right)}{2} \quad (20)$$

where  $t$  is the current time,  $E(t)$  is the input energy,  $E_t$  is the total input energy,  $t_r$  is sunrise time, and  $T_s$  is total sun hours. A "box" is formed by the intersection of dry adiabats (at  $2^\circ\text{C}$  intervals) and isotherms (at  $1^\circ\text{C}$  intervals). In this convention, 1 box (in the lower portion of the Skew T-log p chart) equals  $7 \text{ J kg}^{-1}$ . The diurnal heating which is accounted for by this algorithm is graphically represented by Fig. 6.

Crum and Cahir (1983) note that accurate modifications of the 12 UTC surface dewpoints alone led to favorable results for their investigation. In fact, experiments showed that this one change produced better results than cases where changes were made above the boundary layer. This led them to conclude that it is critically important to use an accurate forecast surface dewpoint for their forecasts.

Schaefer (1975) examined the moisture stratification in the "well-mixed" boundary layer and its temporal changes during the diurnal cycle.

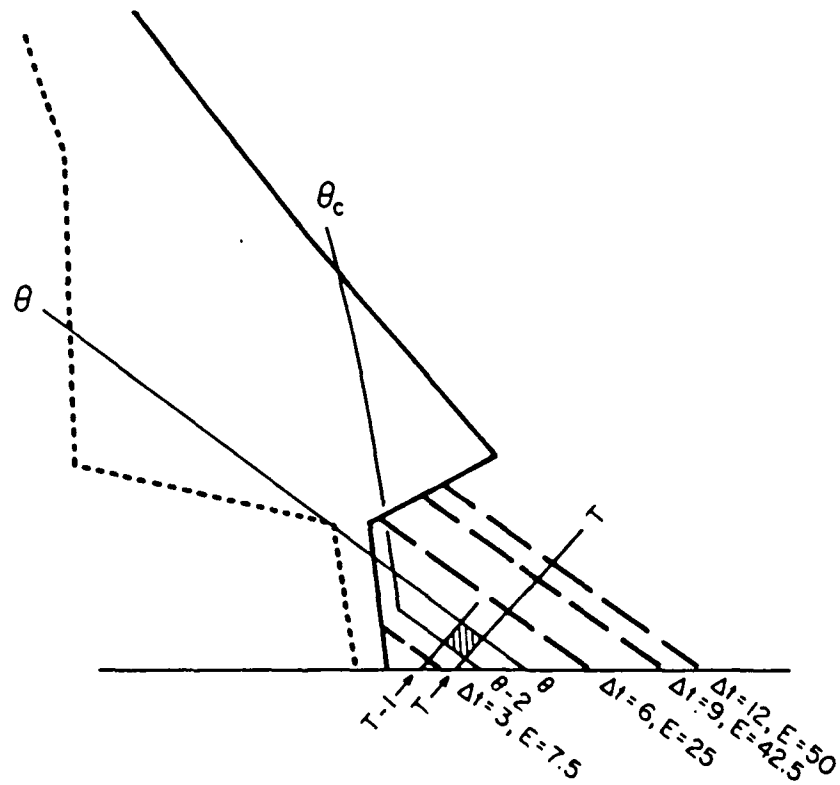


Fig. 6 Idealized energy input by surface heating (shaded area is one energy box). Total heat realized is 50 boxes ( $350 \text{ J kg}^{-1}$ );  $\Delta t$  is time from sunrise. E is energy realized for a given  $\Delta t$  (in boxes). (McGinley 1985)

The quotient of the mean mixing ratio in the lowest 100 mb to the surface mixing ratio,  $R$ , was computed for 251 samples composed of tower and National Weather Service (NWS) soundings. Schaefer found that the mean difference of the quotient between sounding times ( 6 and 12 local) decreased by an average of 10%. In the afternoon it is sensibly constant. From his conclusion, a forecast mean mixing ratio for the mixed layer can be determined knowing the forecast surface dewpoint. The 12 UTC boundary layer dewpoints are then adjusted to the computed afternoon mean mixing ratio.

### 3.3.2 MIDDLE AND UPPER LEVEL CHANGES

Changes to the middle and upper levels can be estimated by first determining the mean geostrophic advection of temperature for a layer from the 12 UTC sounding using the relationship

$$-\overline{\vec{V}} \cdot \nabla_p \overline{T} = \frac{-2fA}{R \ln p_l / p_u} \quad (21)$$

given the geostrophic wind direction and speed at the top and bottom of the layer,  $\vec{V}_{\text{lower}}$  and  $\vec{V}_{\text{upper}}$ . This method assumes that the winds at and above 700 mb are geostrophic. The area,  $A$ , is determined from

the triangle formed by these two wind vectors and the thermal wind vector derived in the same layer. The Coriolis force,  $f$ , dry air gas constant,  $R$ , and the pressure values,  $P_{upper}$  and  $P_{lower}$ , for the respective wind levels are the other variables.

The forecast temperature value is simply calculated by adding some fraction (15%) of the mean geostrophic temperature advection over a certain number of hours to the original mean temperature from the 12 UTC layer. After the forecast sounding is created it is checked for superadiabatic lapse rates. If any are found, the layers are adjusted according to a scheme by Haltiner and Williams (1980) which conserves the total energy.

#### 3.4 VALIDATION TECHNIQUES

For the purposes of this investigation, it is necessary to apply representative atmospheric profiles to the events which will be used to validate the methodologies. For a hail or wind event to be considered in this investigation, the event must have occurred within 3 hours of sounding time and within 100 km of the rawinsonde launch site. This proximity criteria is similar to that

used to select proximity soundings described by Maddox (1973) and Leftwich (1984). The largest hailstones and strongest gusts recorded in the Storm Data records for a given event were assumed to be representative of the maximum potential severity for that particular storm. This one assumption possibly contributes the largest source of error in this study since both the largest hailstone or strongest gust for a particular storm may not have been observed. In fact, many wind gust entries in the Storm Data records were estimates. Despite possible errors, this investigation assumed the extreme values to be reasonable estimates of ground "truth". Table 2 was used to convert many of the descriptive hail sizes to specific diameters.

The primary field experiment data considered are;

1. PRE-STORM, conducted in the Kansas-Oklahoma area from 1 May 1985 to 27 June 1985.
2. AVE-SESAME I, conducted in the Texas-Oklahoma area 10-11 April 1979.
3. AVE-SESAME II, conducted in the Texas-Oklahoma area 19-20 April 1979.

Penny - 3/4" diameter  
Dime - 3/4" diameter  
Nickel - 1" diameter  
Quarter - 1" diameter  
Anthony dollar - 1 1/4" diameter  
Half dollar - 1 1/4" diameter  
Walnut - 1 1/2" diameter  
Golfball - 1 3/4" diameter  
Hen egg - 2" diameter  
Tennis ball - 2 1/2" diameter  
Baseball - 2 3/4" diameter  
Tea cup - 3" diameter  
Grapefruit - 4" diameter  
Softball - 4 1/2" diameter

Table 2 Conversion table of descriptive hail sizes to actual measured diameters.  
(Doswell 1985)

Since the majority of the soundings used during Fawbush and Millers' investigation were from the Midwest, soundings from other sections of the country such as the Northeast, Southeast, etc. were included in the study. Storm Data records were used to identify possible hail and wind events.

The final validation procedure for the hail algorithm examines composite hailstorm soundings calculated by Fawbush and Miller (1953). Fawbush and Miller examined composite soundings for air masses which produced one-half, one, and four inch hail. For each composite sounding, the data will be used to verify the proposed hail methodology in two respects: the composite soundings will be applied to the algorithms for (1) verification purposes, and (2) to perform a sensitivity check on the variables used in computing hail size such as the drag coefficient, density of hail, and level of hail formation.

Validation of the forecast sounding required applying the algorithm to a 12 UTC sounding which precedes a hail/wind event and satisfies the hail/wind proximity sounding requirements. Estimates of hail and wind from the forecast

sounding were compared with estimates obtained from the proximity soundings.

### 3.5 THE SOUNDING ANALYSIS PACKAGE

Accurate prediction of hail size and thunderstorm surface wind gusts require a forecaster's ability to first determine the likelihood of convection. Understanding the characteristics of the atmosphere, such as the stability, positive energy, presence of a lid, and equilibrium level, etc., for both the 12 UTC profile as well as the forecast sounding will aid the forecaster in this determination. In addition to estimated potential hail size and thunderstorm surface wind gust velocities, various stability parameters are routinely available as part of the sounding analysis algorithm to assess the probability of convection as well as to prognose the degree of severity (Table 3). These additional thermodynamic variables were used in this study to help understand the structure of the sounding as well as to determine the significance and utility of the forecast sounding. Appendix A describes how each of the parameters in Table 3 are computed.

K Index  
Total-Totals Index  
Sweat Index  
Showalter Index  
Lifted Index  
SELS Lifted Index  
Best Lifted Index  
LID Strength Index  
Lifted Condensation Level  
Level of Free Convection  
Convective Condensation Level  
Equilibrium Levels (CCL and LFC based)  
Height of the Wet-Bulb Zero  
Positive Area based on the CCL  
Negative Area based on the CCL  
Bulk Richardson Number  
Convective Available Potential Energy  
Convective Inhibition  
Convective Temperature  
Precipitable Water  
Potential Hailstone Diameter (LFC based)  
Potential Hailstone Diameter (CCL based)  
Potential Surface Wind Gust Velocity

Table 3 Parameters calculated by the sounding analysis algorithm.

#### 4. RESULTS AND DISCUSSION

A sounding analysis was completed for each proximity sounding in this study, an example of which is shown in Table 4. Each analysis includes hail estimates computed by the updated Fawbush-Miller hail technique (AWS TR-200) and the Pino-Moore hail algorithms (CCL and LFC) along with computed wind gusts based on Fawbush-Miller (AWS TR-200), Foster (1958), and Anthes (1977). In addition to these estimates, various stability parameters and thermodynamic energy values relative to each atmospheric profile are included. Appendix A briefly describes the method for computing each parameter.

For each sounding analysis, two hail size estimates are calculated from the Pino-Moore algorithms, based on the positive areas above the LFC and the CCL. If the surface temperature for each proximity sounding was within  $2^{\circ}\text{F}$  of the convective temperature or greater and the lid strength term was less than or equal to  $2^{\circ}\text{C}$ , the hail stone size estimate calculated from the CCL was used. Graziano and Carlson (1988) found a practical threshold for convective penetration of the lid

SI = -5.0  
KI = 37.5  
LI = -4.9  
BEST LIFTED INDEX = -4.5  
SELS LI = -999.0  
MAX TEMP BASED ON SELS LI = -999.0 deg F

SWEAT INDEX = 325.6  
TTI = 53.7  
LID STRENGTH = 1.01

THE CONVECTIVE TEMP BASED ON THE CCL = 76.0 deg F  
The CCL is at 850.0 mb  
The EL (CCL based) is at 202.4mb -54.2 deg C  
The LCL(BL) is at 833.3 mb  
The LFC is at 819.0 mb 13.4 deg C  
The EL (LFC based) is at 213.0 mb -54.3 deg C  
CONVECTIVE AVAILABLE POTENTIAL ENERGY = 1680.5 J/kg  
CONVECTIVE INHIBITION = 12.5 J/kg  
VERTICAL WIND SHEAR (6000 M - 500 M) = 3.7X e-03 s-1  
BULK RICHARDSON NUMBER = 8.3  
POSITIVE AREA (CCL BASED) = 2622.4 J/kg  
NEGATIVE AREA (CCL BASED) = 3.0 J/kg

PRECIPITABLE WATER = 1.13 in  
HEIGHT WET BULB ZERO (AGL) = 9534.9 ft  
W MAX BASED ON LFC = 24.18 m/s  
DIAM OF HAIL FROM LFC = 5.09 cm ( 5.23 cm)  
W MAX BASED ON CCL = 31.03 m/s  
DIAM OF HAIL FROM CCL = 8.35 cm ( 8.44 cm)  
DIAM OF HAIL (TR-200) = 4.23 cm ( 4.23 cm)  
SFC WIND GUST BASED ON F-M = 74.9 kts  
SFC WIND GUST BASED ON FOSTER = 72.4 kts  
SFC WIND GUST BASED ON ANTHES = 40.2 kts

Table 4 Example of the Pino-Moore sounding analysis. Note: for hail sizes, estimates in parentheses are values prior to melting.

occurs at a lid strength of  $2.0^{\circ}\text{C}$ . If these criteria were not met, the LFC estimate was used.

#### 4.1 HAIL SIZE FORECAST VALIDATION

##### 4.1.1 COMBINED CASES

Fifty-eight cases selected from PRE-STORM, AVE-SESAME I, AVE-SESAME II and events from July and August 1986 were used in validating the hail algorithms. Figures 7 and 8 contain the results of the computed hailstone diameters according to the Pino-Moore and Fawbush-Miller methods compared with the observed hailstones. Also shown with each scatter diagram are statistical analyses which include the linear regression equation, the means of the observed and estimated values ( $\bar{x}$  and  $\bar{y}$ ), the standard deviations ( $\text{std-dev } x$  and  $\text{std-dev } y$ ), the scatter, the correlation coefficient ( $r$ ), the bias, and the Student-t statistic value for both sets of data.

Comparing Figure 7 and 8, the Pino-Moore algorithm proved to be much more successful in estimating the actual size of the hail events. The set of data represented in Fig. 7 resulted in a Student-t statistic significant at the 0.5% level

$y = 3.1535 + 0.3889x$  is regression eqn  
 $\bar{x} = 5.2034$   
 $\bar{y} = 5.1771$   
 $\text{std-dev } x = 2.3617$   
 $\text{std dev } y = 1.8234$   
 $\text{scatter} = 1.5616$   
 $r = 0.5037$   
 $\text{Bias} = 0.99$   
 $\text{Student-t} = 4.36$   
 $N = 58$

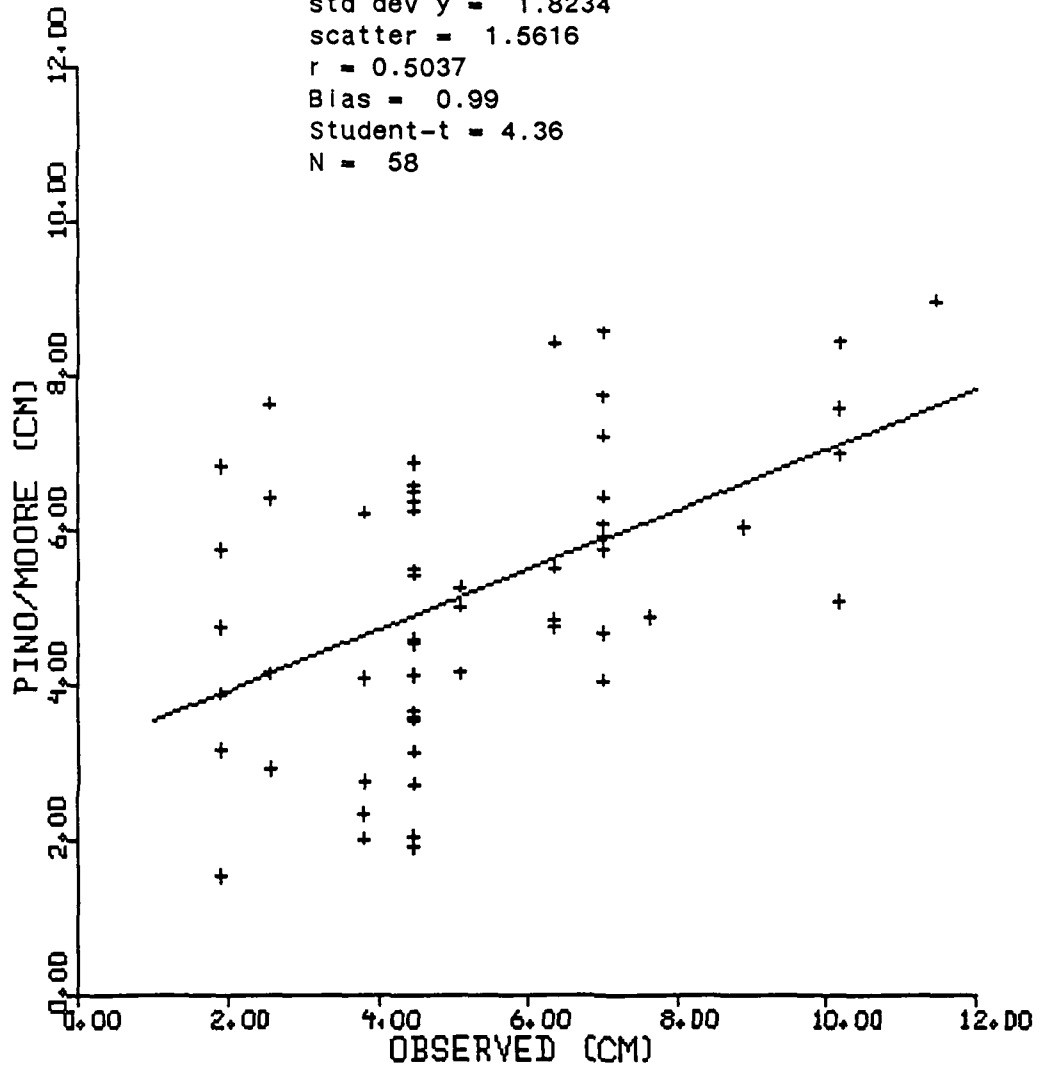


Fig. 7 Scatter diagram with statistical analysis for Pino-Moore hail diameter estimates versus observed hail diameters.

$y = 1.6357 + 0.1254x$  is regression eqn  
 $\bar{x} = 5.2034$   
 $\bar{y} = 2.2879$   
 std-dev  $x = 2.3617$   
 std dev  $y = 1.5620$   
 scatter = 1.5204  
 $r = 0.1895$   
 Bias = 0.44  
 Student-t = 1.44  
 $N = 58$

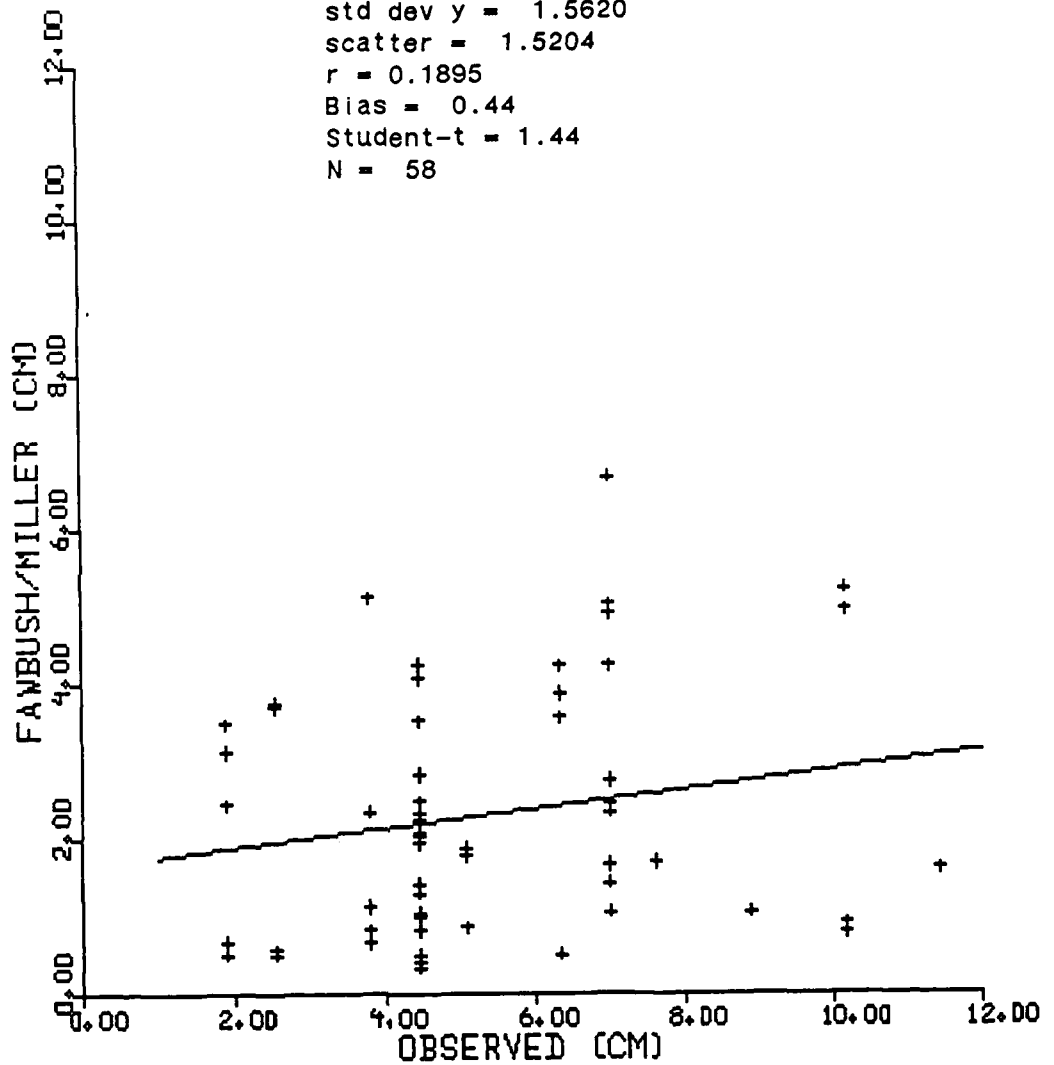


Fig. 8 Scatter diagram with statistical analysis for Fawbush-Miller hail diameter estimates versus observed hail diameters.

whereas the data represented by Fig. 8 resulted in a Student-t statistic significant at the 10% level. Additionally, the Fawbush-Miller method did not indicate severe storm potential (greater than 1.91 cm) for 24 of the 58 cases studied while the Pino-Moore algorithm missed only one of the 58 cases.

These results raise doubt as to the validity of Fawbush and Miller's (1953) statement that "hailstones maintain their size for at least 9000 feet of freefall, after which rapid melting and disintegration take place". Some of the error in determining hailstone size with the Fawbush-Miller technique can be attributed to the way the positive area is calculated (Fig. 1). Their triangle method only approximates the actual positive area. However, the results obtained in this study suggest that their premise concerning rapid melting and disintegration may not be as significant or dramatic as they state.

Melting rates obtained from the Pino-Moore method varied from approximately 5% for the largest stones to as much as 100% for stones less than 1 cm in diameter. These results are in agreement with those reported by Mason (1956), Macklin (1963), and

Auer and Marwitz (1972). While Fawbush and Miller suggest dramatic melting for large hailstones with a corresponding WBZ height greater than 10,500 feet, our algorithm indicates that these larger stones undergo the least amount of melting of any of the hailstones. As the size of the stone decreases, melting rates increase. Hailstones initially having diameters less than 1 cm at the level of hail formation very seldom reach the surface even though these stones fall within the storm's protective downdraft.

The results of the Fawbush-Miller method was statistically analyzed disregarding their correction due to melting (Fig. 9). The linear regression equation, correlation coefficient (.22 vs. .19), bias (.76 vs. .44), and the t-statistic (significant at the 5% level) all indicate that the Fawbush-Miller technique produced better estimates for the 58 cases in this study when melting was neglected. In addition, the Fawbush-Miller method indicated severe potential for 49 of the 58 cases missing only 9 severe situations.

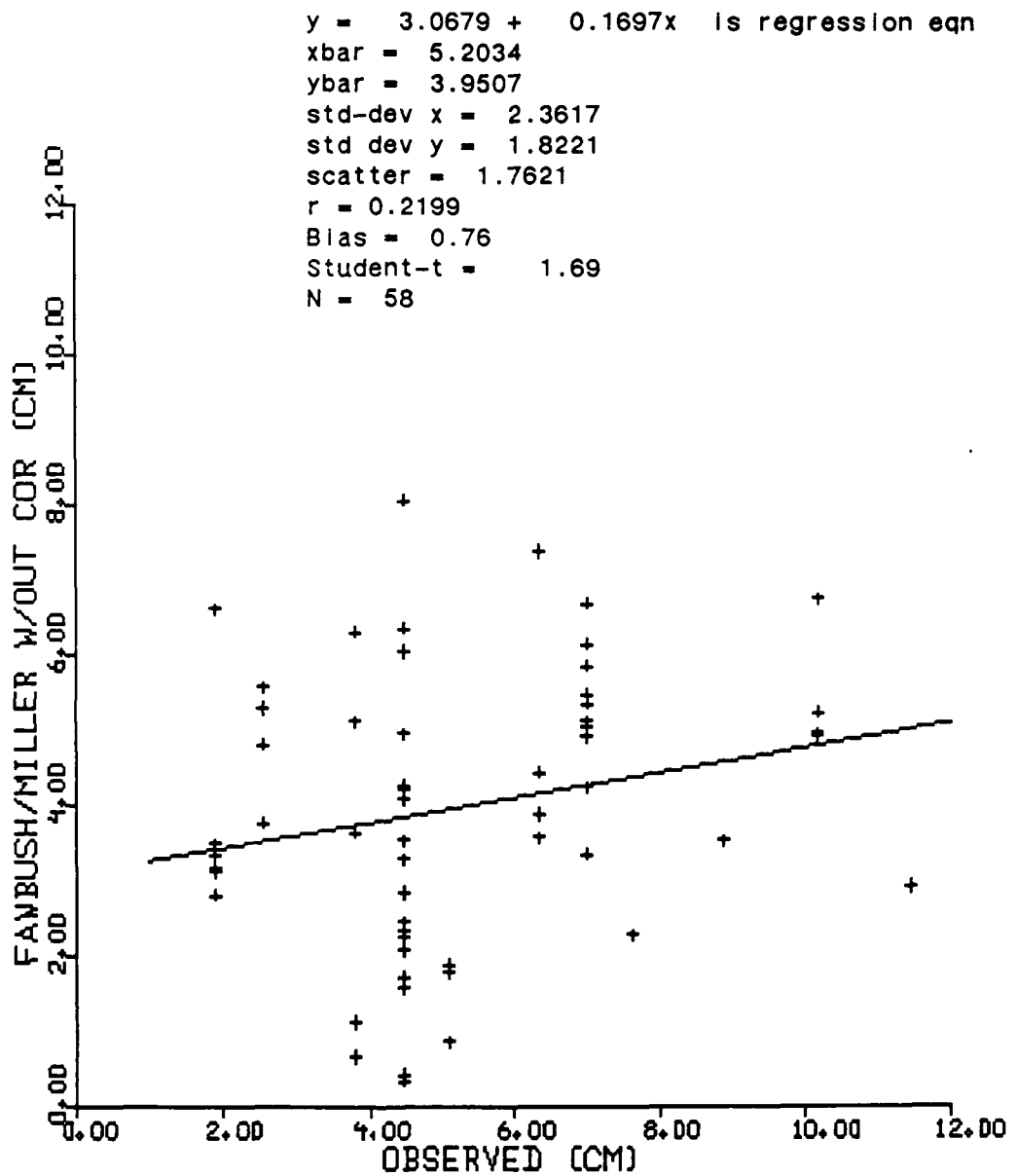


Fig. 9 Scatter diagram with statistical analysis for Fawbush-Miller hail diameter estimates without melting.

## 4.1.2 COMPOSITE SOUNDINGS

Fawbush and Miller's (1953) hail study produced composite soundings for one-half inch, one inch, and four inch hail (Fig. 10, 11, 12). The dewpoint profile for each of these composite soundings had to be calculated since the soundings contained in their original paper included only the mean temperature and wet-bulb curves. Heights were hydrostatically computed. Table 5 shows the results of the calculated hailstone sizes for each of the soundings. Since no other synoptic data was included with these composite soundings and since the convective temperatures for each of the soundings were fairly high, much higher than the surface temperatures of the soundings, the hailstone sizes computed by the LFC-based CAPE were taken as being representative of the storms which developed under these thermodynamic conditions.

As indicated in Table 5, values computed by the Pino-Moore algorithm for the four inch and one inch composite soundings were closer to the observed hailstone values than those estimated by Fawbush-Miller. Both methods did poorly in the estimates for the half-inch composite sounding. One reason

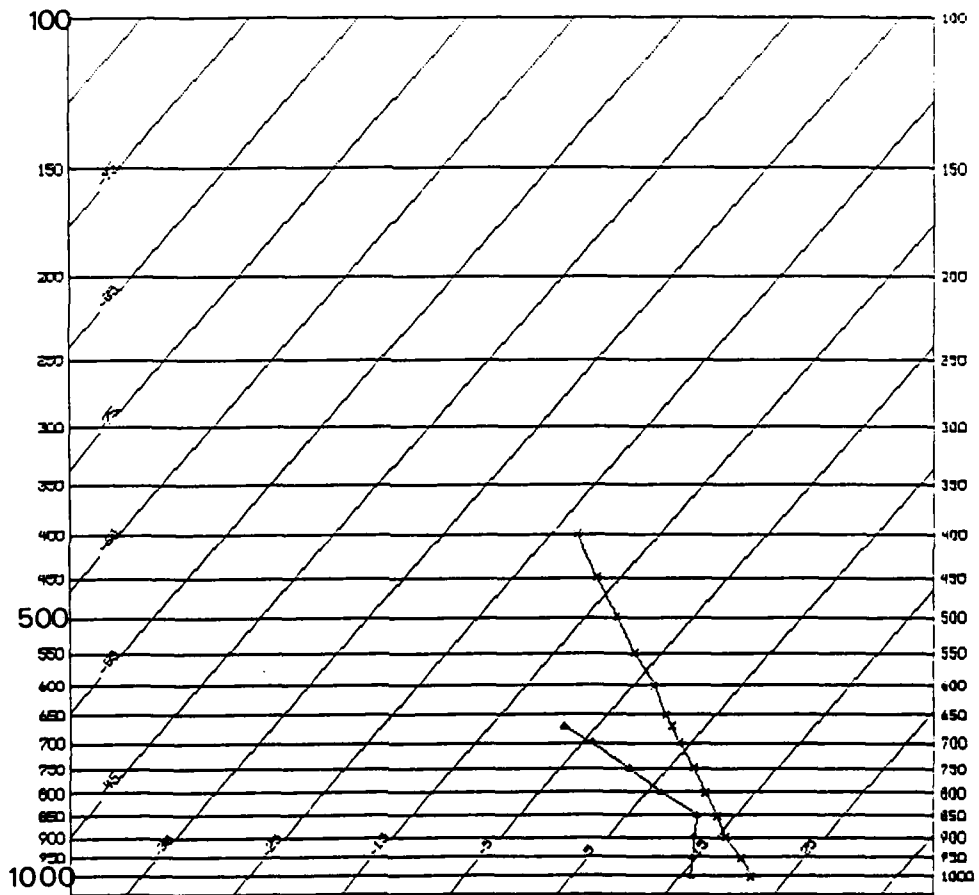


Fig. 10 Mean temperature and dewpoint temperature for air masses producing hailstones 1/2 inch in diameter, 68 cases. (Fawbush and Miller 1953)

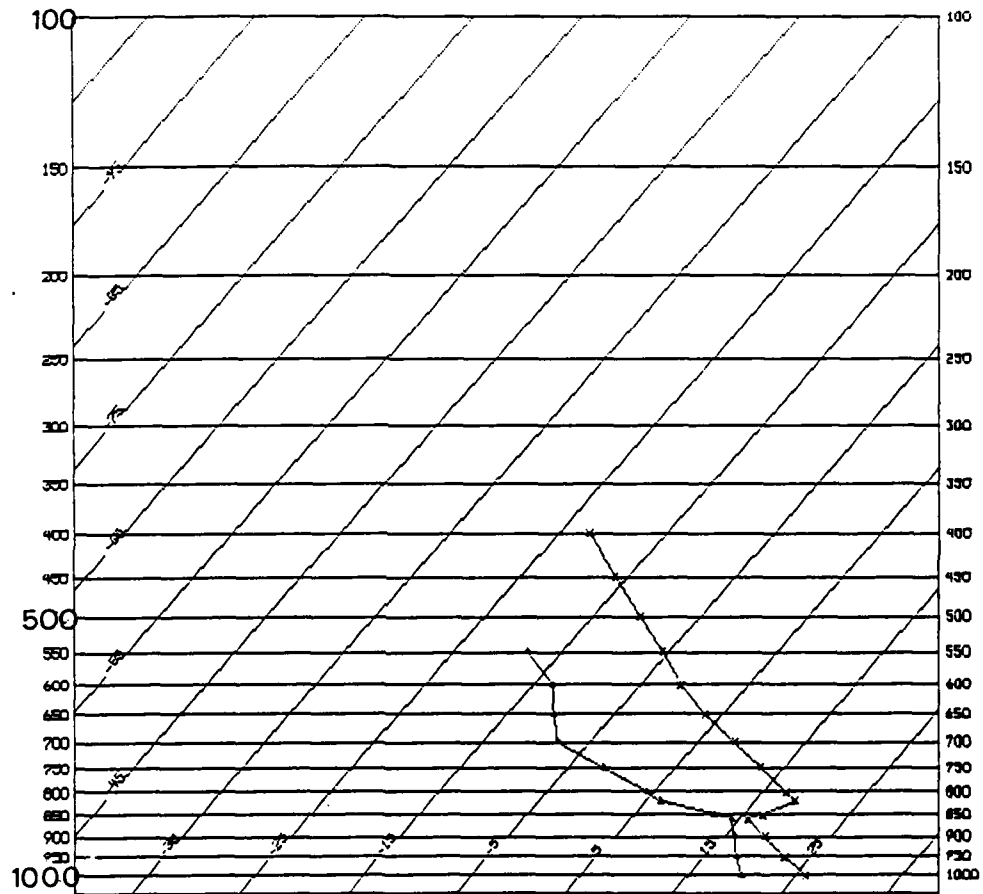


Fig. 11 Mean temperature and dewpoint temperature for air masses producing hailstones 1 inch in diameter, 25 cases. (Fawbush and Miller 1953)

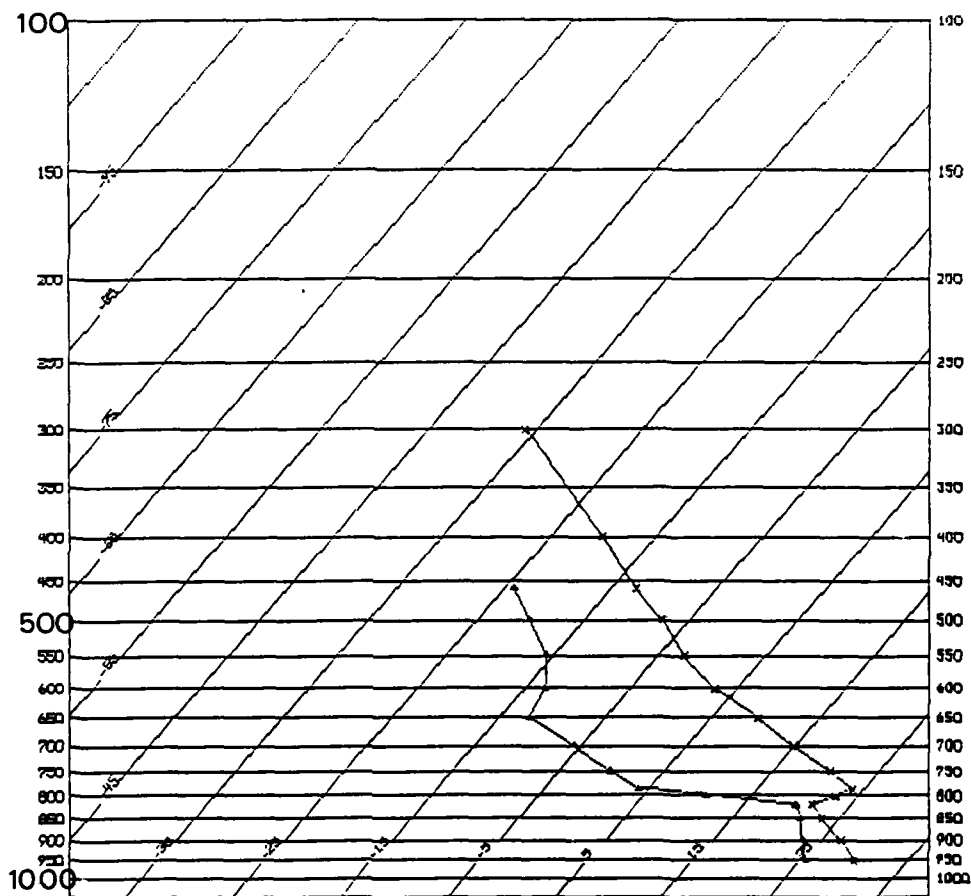


Fig. 12 Mean temperature and dewpoint temperature for air masses producing hailstones 4 inches in diameter, 2 cases. (Fawbush and Miller 1953)

	FAWBUSH-MILLER	PINO-MOORE
	DIAMETER/ERROR	DIAMETER/ERROR
HALF-INCH COMPOSITE (1.27 cm)	2.45 (+1.18)	0.17 (-1.10)
ONE-INCH COMPOSITE (2.54 cm)	3.24 (+0.70)	3.13 (+0.59)
FOUR-INCH COMPOSITE (10.16 cm)	3.11 (-7.01)	12.27 (+2.11)

Table 5 Results of the composite sounding hail size estimates as computed by Pino-Moore and Fawbush-Miller techniques.

why the Pino-Moore method underestimated the half-inch composite sounding could be attributed to our assumption of the drag coefficient being 0.6. As Matson and Huggins (1980) found in their study, small hailstones in this range may exhibit larger drag coefficients because of the increase in the irregularity of the hailstone shapes. The sounding analysis was recomputed with a drag coefficient of 0.87 and the Pino-Moore method resulted in a hailstone diameter of 0.68 cm after the effects of melting.

In light of these results, the Pino-Moore method should be tested for hail events less than 1.91 cm. It was not tested in this study since the hail events were all greater than 3/4 of an inch in diameter. A future test should determine which drag coefficient, 0.60 or 0.87, results in the best estimates. If the test shows in favor of a drag coefficient of 0.87 for observed hailstones less than 1.91, the algorithm could easily be modified to allow a value of 0.87 for small hailstones and 0.60 for hailstones greater than 1.91 cm.

#### 4.2 CONVECTIVE WIND GUST VALIDATION

Similar to the hail size validation, three techniques for estimating convective wind gusts were tested for 47 cases (Fig. 13, 14, 15). The observed wind gusts were identified from the Storm Data records. For a significant number of cases, the wind gusts were reported as estimates. Although a statistical analysis was completed for each set of data, the results of these analyses were questionable due to; (1) the small range of observed values, (2) the uncertainty of the representativeness of the observed gusts to the actual severity of the storms which produced them, and (3) the fact that some of the validating gust speeds were estimates.

Statistical analyses aside, one striking feature evident in the Fawbush-Miller and Foster scatter diagrams is the amount of vertical scattering. This raises some doubt as to the operational utility of these methods. While results of the Anthes' method seem to underforecast convective gust events slightly (bias = 0.96) compared to the significant overforecasting of the other techniques (bias = 1.29, 1.23), the Anthes'

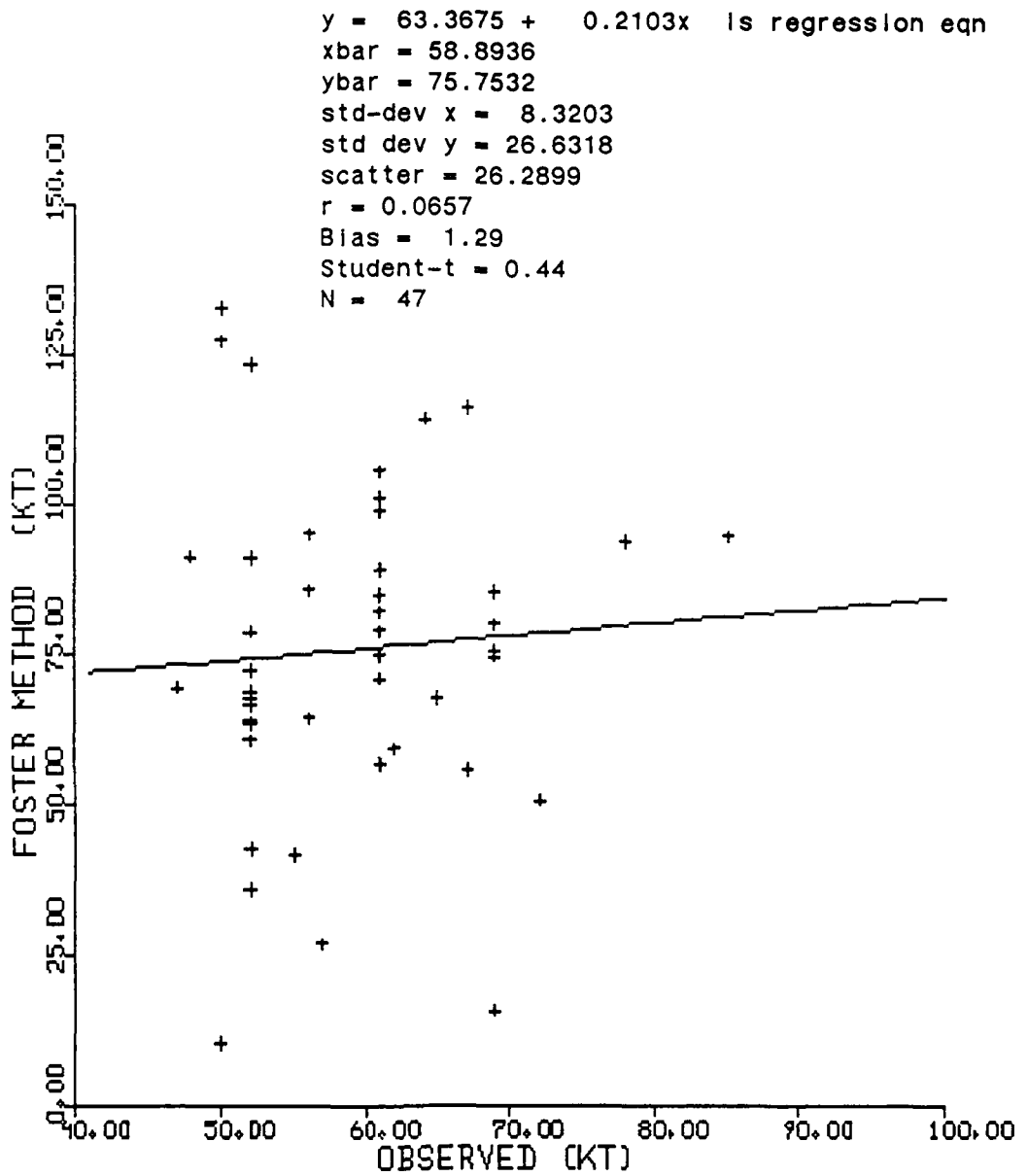


Fig. 13 Scatter diagram with statistical analysis for winds estimated by Foster method versus observed wind gusts.

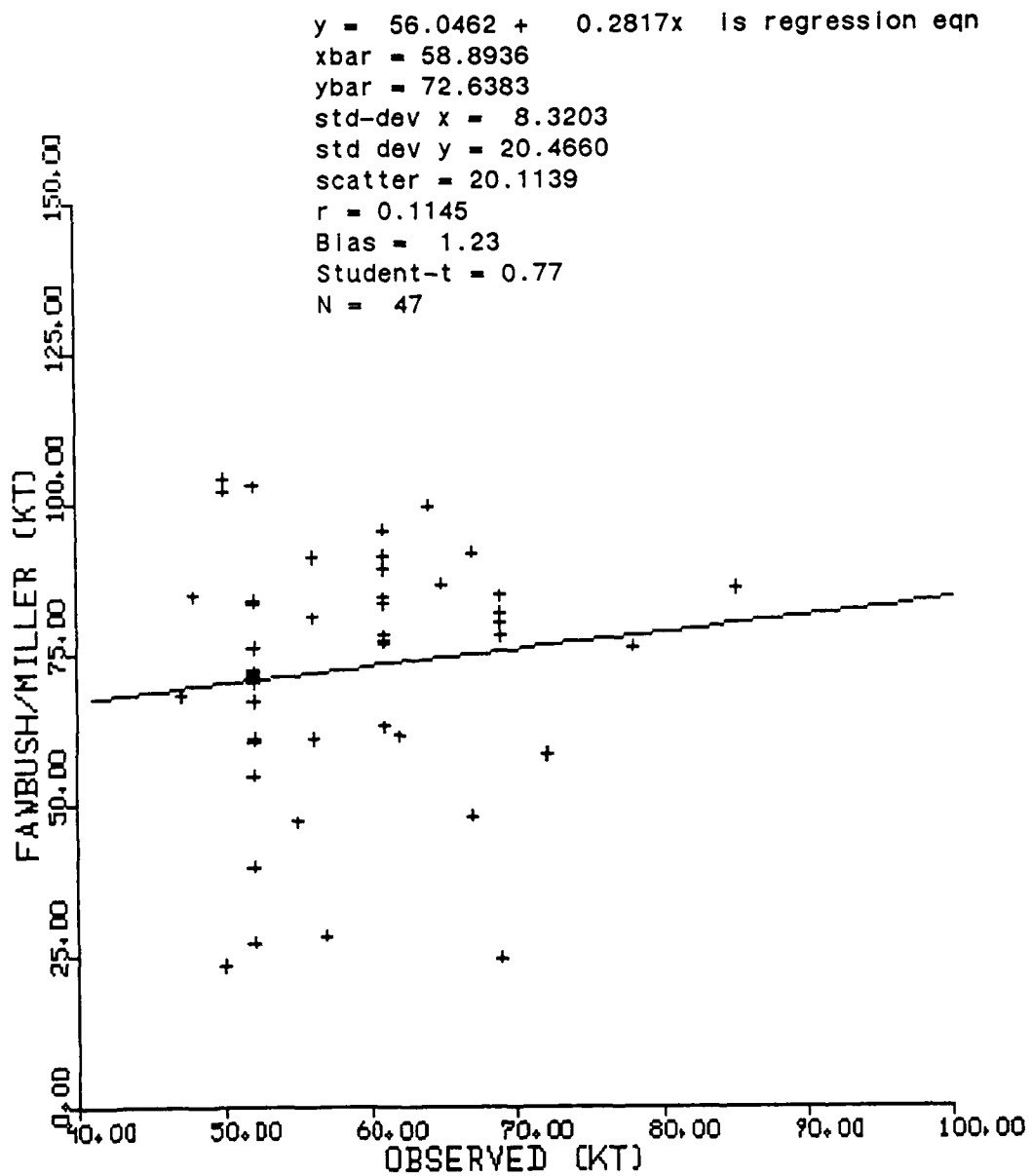


Fig. 14 Scatter diagram with statistical analysis for winds estimated by Fawbush-Miller method versus observed wind gusts.

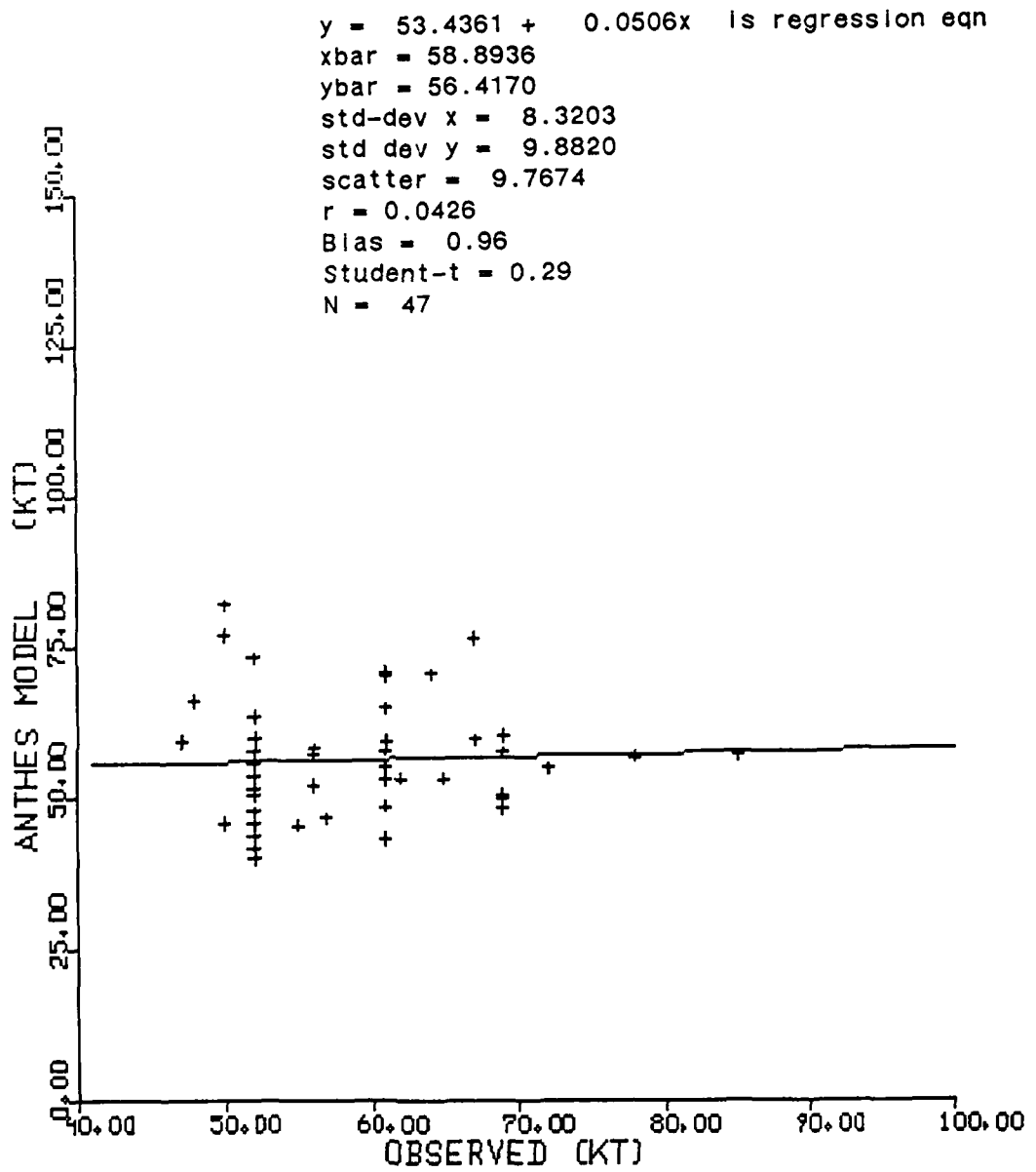


Fig. 15 Scatter diagram with statistical analysis for winds estimated by Anthes method versus observed wind gusts.

technique displays considerably less scatter. Based on scattering alone, the Anthes method seems to offer more reliability in an operational setting.

A possible reason for the Anthes' method underestimation of the winds lies in the algorithm's neglect of the water-loading term above the LFS. The integration of all three terms in Anthes' vertical velocity equation assumes no contribution of any of the terms above the LFS. Precipitation fallout from above the LFS into the forming downdraft would result in strengthening the downdraft.

#### 4.3 SENSITIVITY STUDY OF KEY VARIABLES

The values of the hailstone drag coefficient, density, and the level of hail formation used in the Pino-Moore method were taken from a wide range for values offered by the various literature reviewed. While the results of this study appear to be well supportive of our values of these variables, the author wanted to show the importance of these variables to the resultant hail estimates. Table 6 shows the wide range of hail estimates obtained by varying the hailstone drag coefficient, density, and

#### DRAG COEFFICIENT

(density of ice = 0.90)  
(level of hail formation  $T_p = -10^\circ\text{C}$ )

0.45*	(smooth sphere)	5.74 cm
0.60*	(rough sphere)	7.74 cm
0.70		9.05 cm
0.87	(Matson and Huggins)	11.29 cm

#### DENSITY OF HAILSTONE

(drag coefficient = 0.60)  
(level of hail formation  $T_p = -10^\circ\text{C}$ )

0.70 g cm <sup>-3</sup>	(Foster and Bates)	9.99 cm
0.89 g cm <sup>-3</sup> *	(Matson and Huggins)	7.82 cm
0.90 g cm <sup>-3</sup>		7.74 cm
0.92 g cm <sup>-3</sup>		7.56 cm

#### LEVEL OF HAIL FORMATION

(drag coefficient = 0.60)  
(density of ice = 0.90 g cm<sup>-3</sup>)

$T_p = -5.0^\circ\text{C}$	6.68 cm
$T_p = -10.0^\circ\text{C}$ *	7.74 cm
$T_p = -15.0^\circ\text{C}$	8.63 cm

\* = Values used by Pino-Moore

Table 6 Hailstone diameters computed by varying drag coefficient, hailstone density, and level of hail formation.

level of hail formation. This sensitivity study was applied to the 0000 UTC May 27<sup>th</sup>, 1986 Enid, Oklahoma sounding obtained during PRE-STORM. The verifying hailstone size for this particular sounding was 6.99 cm.

As indicated by Table 6, increasing the drag coefficient from 0.60 to 0.87 (a 45% increase) results in about a 46% increase in hail diameter. This one variable alone demonstrates the high sensitivity inherent with the Pino-Moore algorithm. Increasing the density of the hailstone from  $.70 \text{ g cm}^{-3}$  to  $0.92 \text{ g cm}^{-3}$  (31%) decreases the diameter 24%. A diameter increase of 29% results from raising the level of hail formation from  $-5.0^{\circ}\text{C}$  to  $-15.0^{\circ}\text{C}$ .

#### 4.4 FORECAST SOUNDING UTILITY

Fifteen 1200 UTC soundings were identified during the validation of the hail methodologies as possible test cases for the forecast sounding validation. These soundings preceded an afternoon/early evening hail event for which a proximity sounding was available. Sounding analyses were performed on: (1) the unadjusted 1200 UTC

sounding, (2) an adjusted 1200 UTC sounding considering diurnal changes in the mixed layer, and (3) a forecast sounding adjusting both the mixed layer as well as the middle and upper layers.

In adjusting the diurnal changes in the mixed layer, the algorithm requires the operator's input of several parameters. The algorithm asks the operator for:

- (1) the current date,
- (2) the modification factor (Table 1),
- (3) the station's latitude and longitude,
- (4) the number of hours past sunrise convection is expected.

Based on this input, the algorithm computes the forecast surface temperature for the time of convection. The program then indicates this temperature. If the operator does not agree with this estimate, the operator may input his/her own temperature. Based on the temperature input into the program, the lowest part of the sounding is adjusted to account for this energy as shown earlier in Fig. 6. The algorithm then asks for the expected surface dewpoint at time of convection. This dewpoint is used in adjusting the moisture profile in the mixed layer. If an inversion is present just

above the mixed layer, the surface dewpoint is adjusted and moisture lapse rate in the mixed layer is not adjusted. This condition is addressed in section 4.4.1. The top of the mixed layer is determined during the thermal adjustment portion of the algorithm. In validating the adjusted soundings, the surface temperature and dewpoint temperature of the corresponding proximity sounding was used.

Table 7 contains the results of the hailstone diameter estimates based on the various adjusted and unadjusted soundings. A surprising result indicated by the mean errors is that while the proximity sounding underestimated the diameters by 1.18 cm, both adjusted soundings produced better mean errors than the proximity soundings as well as the 1200 UTC soundings. An example of the decision making process associated with using the forecast sounding algorithm is given in section 4.4.

Of the fifteen soundings analyzed in this section, two were associated with strong convective gust events. Both 1200 UTC sounding analyses did not indicate potential for convectively-driven downdraft gusts for all three techniques. For the

OBSERVED	1200UTC	FCSTRAOB BDY ONLY	FCSTRAOB BDY + GEO	PROXIMITY
3.81	0.00(-3.81)	4.11(+0.30)	5.60(+1.79)	2.75(-1.06)
6.35	1.71(-4.64)	3.58(-2.77)	4.16(-2.19)	8.43(-2.08)
4.45	8.04(+3.59)	7.12(+2.67)	7.70(+3.25)	6.48(-2.03)
10.16	2.62(-7.54)	4.94(-5.22)	6.74(-3.42)	5.08(-5.08)
4.45	4.61(+0.16)	4.82(+0.37)	5.20(-0.75)	3.60(-0.85)
8.89	4.39(-4.50)	5.40(-3.49)	N/A	6.04(-2.85)
6.35	2.36(-3.99)	5.35(-1.00)	6.36(+0.01)	4.83(-1.52)
6.99	2.94(-4.05)	5.55(-1.44)	6.63(-0.36)	5.92(-1.07)
3.81	3.67(-0.14)	3.86(+0.05)	4.46(-0.65)	4.08(+0.27)
4.45	1.98(-2.47)	5.14(+0.69)	4.77(+0.32)	6.38(+1.93)
3.81	1.98(-1.83)	6.58(-2.77)	6.30(+2.49)	2.33(-1.48)
4.45	0.00(-4.45)	2.38(-2.07)	2.46(-1.99)	3.56(-0.89)
3.81	0.14(-3.67)	0.76(-3.05)	3.89(+0.08)	2.02(-1.79)
6.35	6.85(+0.50)	6.09(-0.26)	4.60(-1.75)	4.75(-1.60)
4.45	8.86(+4.41)	7.79(+3.34)	8.10(+3.65)	6.87(+2.42)
TOTAL ERROR	(-32.43)	(-14.65)	(+0.48)*	(-17.68)
MEAN ERROR	(-2.16)	(-0.98)	(+0.03)*	(-1.18)

\* Total and mean error for 14 cases only.

Table 7 Validation results for the forecast sounding algorithm. Numbers in parentheses indicate error.

forecast soundings which included geostrophic thermal advection, severe wind gust potential was indicated by the Fawbush-Miller and the Foster techniques while the Anthes technique favored severe potential for one of the cases with near severe threshold for the second case. The proximity soundings indicated severe potential for all three techniques.

#### 4.4.1 LIMITATIONS AND WEAKNESSES

While the forecast sounding proved its utility for severe events where dynamics played an overwhelming role in the development of the severe convection, interrogation of the resultant forecast soundings as compared to the corresponding proximity sounding revealed several weaknesses with the forecast sounding algorithm. In situations where very little heating took place, the adjusted sounding resulted in a very shallow mixed layer. This in turn allowed for geostrophic thermal advection to occur at low levels which was usually too strong. In similar situations where an inversion was present just above the adjusted mixed layer, the adjusted moisture structure of the mixed layer as computed by Schaefer (1975) resulted in

too dry a layer. To correct for this, the algorithm was modified to "look" for the presence of an inversion (an increase in temperature of at least  $1^{\circ}\text{C}$ ) in the three levels above the mixed layer. If an inversion exists, the algorithm does allow for a change in the surface dewpoint but does not adjust the moisture lapse rate in the mixed layer.

The diurnal heating algorithm is best suited for quiescent surface conditions in which there is weak or little low level thermal advection. In some of the cases, especially during the early spring months, low level cold air advection inhibited the solar diurnal heating. The predicted maximum surface temperature was approximately  $5^{\circ}\text{C}$  too warm. Although low level cold air advection can lead to overestimation of the effects of diurnal heating, low level warm air advection does not seem to affect the solar heating significantly.

During the summer months, the role of the geostrophic thermal advection in the modification of the upper air thermal structure may not be as prominent as during the spring months. The final version of the algorithm accounts for these situations and allows the operator to neglect this

advection.

Applying 12 hour forecast changes to the middle and upper levels using the geostrophic thermal advection assumes the wind profile over these levels does not change very much. In reality, however, the wind profile, especially during the spring months, may undergo considerable changes. As a result, estimates of the geostrophic thermal advection may be best applicable when forecasting changes for a only few hours, say 4-6 hours.

#### 4.5 CASE STUDY

On 20 February 1989, severe thunderstorms battered eastern Louisiana and western Mississippi during the late afternoon and early evening hours. In addition to spawning tornados and producing damaging downdraft winds, large hail accompanied these storms. Hail estimated at 2 inches (5.08 cm) fell at Vicksburg, Mississippi. To further illustrate the operational utility of the Pino-Moore sounding analysis and the forecast sounding algorithm, a case study of the hail event at Vicksburg was completed after-the-fact.

An analysis was performed for the 1200 UTC 20 February sounding (Fig. 16) for Jackson, Mississippi. This sounding meets the proximity sounding requirements for this hail event. The 983 mb level data was deleted as it appeared inconsistent. Table 8 is the sounding analysis of Fig 16. The morning Lifted Index was fairly high not indicative of deep convection. The Pino-Moore hail algorithm estimated possible hail of nearly 3/4 inch diameter, assuming a convective temperature of 77°F was reached. The Fawbush-Miller technique estimated hail at less than 1/2 inch. Note also that the wind gust estimates for all three techniques did not favor downdraft conditions.

The forecast sounding was run twice, one allowing diurnal changes as well as geostrophic thermal advection while the second run allowed diurnal changes only (Fig. 17 and 18, respectively). To produce the forecast soundings, the following information was interactively input into the algorithm.

1. The date.
2. A modification factor of 0.5 (overcast conditions) since a stratus deck covered

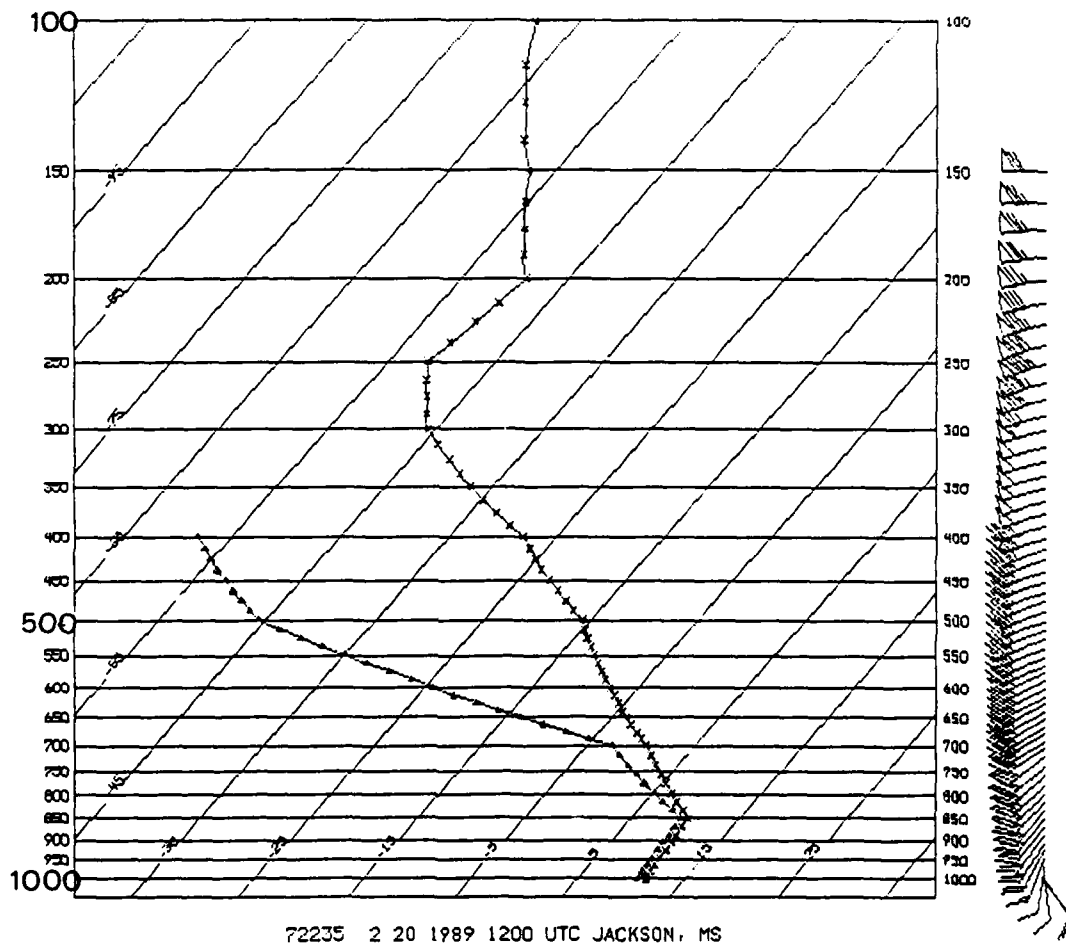


Fig. 16 Upper air sounding for Jackson, MS at 1200 UTC 20 February 1989.

SI = -1.4  
KI = 32.6  
LI = 5.2  
BEST LIFTED INDEX = 3.7  
SELS LI = -999.0  
MAX TEMP BASED ON SELS LI = -999.0 deg F

SWEAT INDEX = 301.9  
TTI = 51.5  
LID STRENGTH = 3.24

THE CONVECTIVE TEMP BASED ON THE CCL = 77.0 deg F  
The CCL is at 824.2 mb  
The EL (CCL based) is at 279.8mb -48.0 deg C  
The LCL(BL) is at 946.6 mb  
The LFC is at -999.0 mb -999.0 deg C  
The EL (LFC based) is at -999.0 mb -999.0 deg C  
CONVECTIVE AVAILABLE POTENTIAL ENERGY = -999.0 J/kg  
CONVECTIVE INHIBITION = -999.0 J/kg  
VERTICAL WIND SHEAR (6000 M - 500 M) = 4.7X e-03 s-1  
BULK RICHARDSON NUMBER = -99.9  
POSITIVE AREA (CCL BASED) = 882.3 J/kg  
NEGATIVE AREA (CCL BASED) = 0.2 J/kg

PRECIPITABLE WATER = 1.02 in  
HEIGHT WET BULB ZERO (AGL) = 9290.6 ft  
W MAX BASED ON LFC = 0.00 m/s  
DIAM OF HAIL FROM LFC = 0.00 cm ( 0.00 cm)  
W MAX BASED ON CCL = 15.77 m/s  
DIAM OF HAIL FROM CCL = 1.64 cm ( 1.83 cm)  
DIAM OF HAIL (TR-200) = 0.92 cm ( 0.92 cm)  
SFC WIND GUST BASED ON F-M = 0.0 kts  
SFC WIND GUST BASED ON FOSTER = 0.0 kts  
SFC WIND GUST BASED ON ANTHES = 0.0 kts

Table 8 Sounding analysis for the 1200 UTC 20  
February 1989 Jackson, MS sounding.

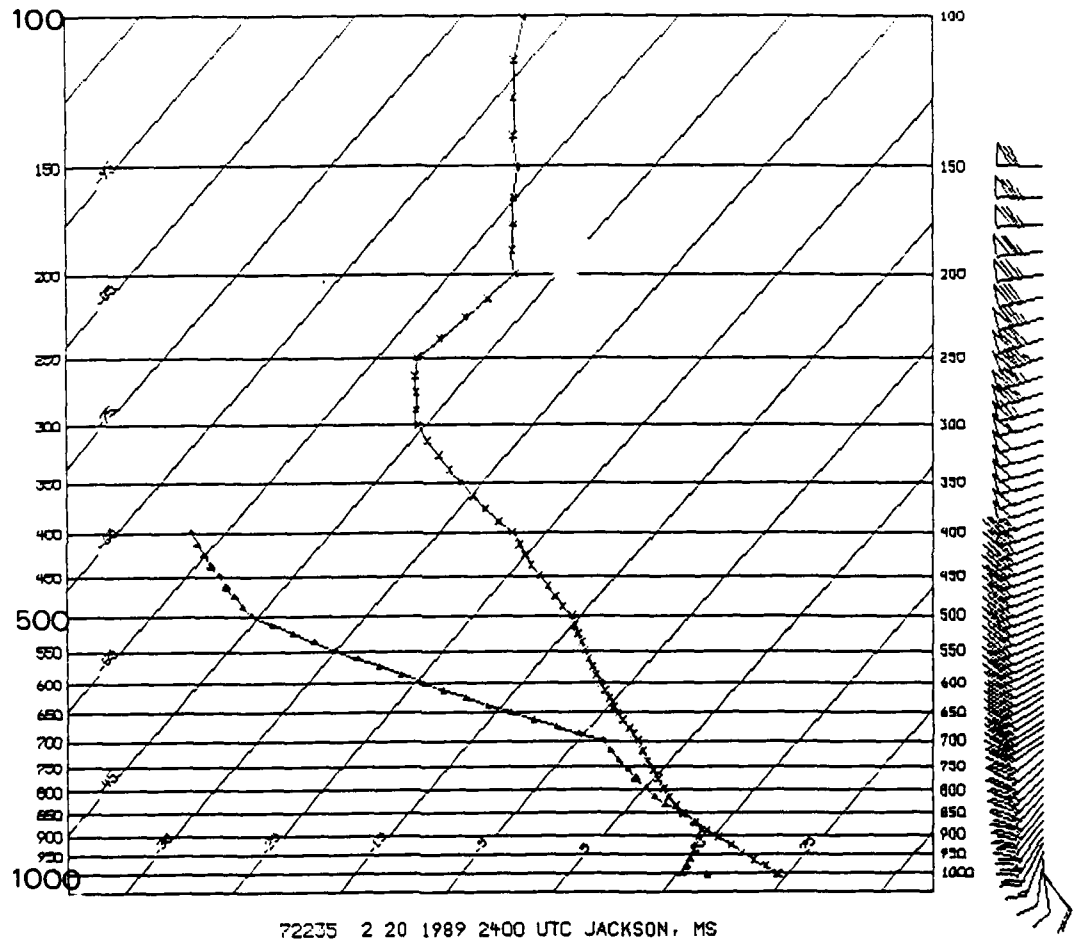


Fig. 17 Forecast sounding (diurnal changes only) for Jackson, MS at 0000 UTC 21 February 1989.

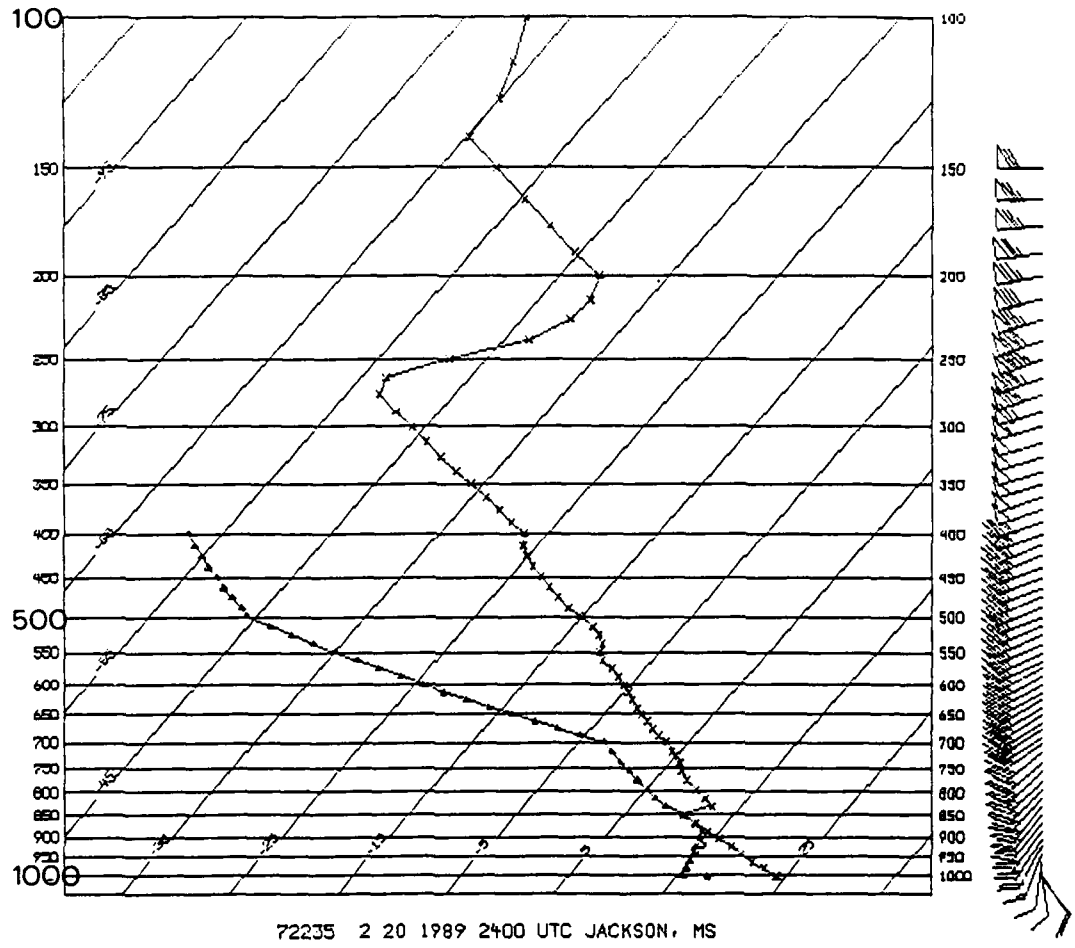


Fig. 18 Forecast sounding (diurnal changes and geostrophic thermal advection) for Jackson, MS at 0000 UTC 21 February 1989.

the region.

3. The station's latitude and longitude.
4. The number of hours expected to time of convection, in this case 12 hours. This was chosen for comparison purposes with the actual 0000 UTC sounding later that evening in addition to the fact that this was the time convection was expected to affect the area.

Based on this information, the forecast sounding computed a surface temperature of 75°F. This value seemed reasonable and was accepted as temperatures did reach the mid 70's that afternoon. A surface dewpoint temperature of 64°F was also input based on the dewpoints advecting into the region. Tables 9 and 10 are the completed sounding analyses for the forecast soundings. These analyses expected a Lifted Index of about -4.4 to -5.0, a decrease of nearly 9.6 to 10.2°C! The CAPE and positive area based on the CCL also were very high for conditions for a winter day during February. More importantly, hail estimates for both techniques now indicated severe potential along with strong downdraft winds. The three operational questions posed for the forecaster to answer are: (1) "Will

SI = -2.1  
KI = 33.5  
LI = -5.0  
BEST LIFTED INDEX = 0.0  
SELS LI = -999.0  
MAX TEMP BASED ON SELS LI = -999.0 deg F

SWEAT INDEX = 329.5  
TTI = 52.4  
LID STRENGTH = 0.00

THE CONVECTIVE TEMP BASED ON THE CCL = 75.7 deg F  
The CCL is at 913.1 mb  
The EL (CCL based) is at 236.7mb -50.6 deg C  
The LCL(BL) is at 886.6 mb  
The LFC is at 885.6 mb 13.9 deg C  
The EL (LFC based) is at 246.2 mb -51.1 deg C  
CONVECTIVE AVAILABLE POTENTIAL ENERGY = 1794.9 J/kg  
CONVECTIVE INHIBITION = 0.4 J/kg  
VERTICAL WIND SHEAR (6000 M - 500 M) = 4.8X e-03 s-1  
BULK RICHARDSON NUMBER = 5.2  
POSITIVE AREA (CCL BASED) = 2606.0 J/kg  
NEGATIVE AREA (CCL BASED) = 0.5 J/kg

PRECIPITABLE WATER = 1.17 in  
HEIGHT WET BULB ZERO (AGL) = 9357.3 ft  
W MAX BASED ON LFC = 27.15 m/s  
DIAM OF HAIL FROM LFC = 4.96 cm ( 5.08 cm)  
W MAX BASED ON CCL = 32.82 m/s  
DIAM OF HAIL FROM CCL = 7.05 cm ( 7.15 cm)  
DIAM OF HAIL (TR-200) = 4.51 cm ( 4.51 cm)  
SFC WIND GUST BASED ON F-M = 57.3 kts  
SFC WIND GUST BASED ON FOSTER = 53.2 kts  
SFC WIND GUST BASED ON ANTHES = 37.1 kts

Table 9 Sounding analysis for the 0000 UTC 21  
February 1989 Jackson, MS forecast  
sounding (diurnal changes only).

SI = -1.5  
KI = 30.4  
LI = -4.4  
BEST LIFTED INDEX = 0.0  
SELS LI = -999.0  
MAX TEMP BASED ON SELS LI = -999.0 deg F

SWEAT INDEX = 305.5  
TTI = 51.2  
LID STRENGTH = 0.00

THE CONVECTIVE TEMP BASED ON THE CCL = 75.7 deg F  
The CCL is at 913.1 mb  
The EL (CCL based) is at 248.5mb -47.7 deg C  
The LCL(BL) is at 886.6 mb  
The LFC is at 885.6 mb 13.9 deg C  
The EL (LFC based) is at 253.2 mb -49.4 deg C  
CONVECTIVE AVAILABLE POTENTIAL ENERGY = 1515.7 J/kg  
CONVECTIVE INHIBITION = 9.6 J/kg  
VERTICAL WIND SHEAR (6000 M - 500 M) = 4.8X e-03 s-1  
BULK RICHARDSON NUMBER = 4.4  
POSITIVE AREA (CCL BASED) = 2287.1 J/kg  
NEGATIVE AREA (CCL BASED) = 0.7 J/kg

PRECIPITABLE WATER = 1.17 in  
HEIGHT WET BULB ZERO (AGL) = 9991.1 ft  
W MAX BASED ON LFC = 21.32 m/s  
DIAM OF HAIL FROM LFC = 2.94 cm ( 3.13 cm)  
W MAX BASED ON CCL = 28.32 m/s  
DIAM OF HAIL FROM CCL = 5.19 cm ( 5.32 cm)  
DIAM OF HAIL (TR-200) = 3.96 cm ( 3.96 cm)  
SFC WIND GUST BASED ON F-M = 53.8 kts  
SFC WIND GUST BASED ON FOSTER = 70.8 kts  
SFC WIND GUST BASED ON ANTHES = 45.1 kts

Table 10 Sounding analysis for the 0000 UTC 21  
February 1989 Jackson, MS forecast  
sounding (diurnal changes plus geostrophic  
thermal advection).

there be thunderstorms later that day?", (2) "Will they reach severe potential?", and (3) "What hail and convective gust estimates should be used as guidance for a hail/wind forecast?". Assuming the forecaster ran the forecast sounding allowing for changes due to diurnal heating and geostrophic thermal advection and performed a sounding analysis as shown herein, how would he or she answer these three questions?

The convective temperature indicated by the sounding analysis indicates 75°F. This was the same surface temperature computed by the forecast sounding algorithm. If the forecaster felt a maximum of 75° was reasonable or if a lifting mechanism was expected during the afternoon hours, the answer to the first question would be yes. Based on the information offered by the sounding analysis, the forecaster could also expect severe weather to accompany the thunderstorms. The third question needs to be answered in order to issue the severe warning. The results shown in Table 10 should be considered as it was shown in section 4.4 that the hail estimates calculated from forecast soundings which allowed geostrophic thermal advection had the lowest mean diameter error. Since

the convective temperature could be reasonably reached, the estimate of 5.19 cm should be used as guidance for issuing the warning. If this estimate was used, he or she would have made good decision since 5.08 cm hail verified. The forecast sounding also indicated strong convective gusts nearing severe threshold ( $> 55$  knots) criteria as estimated by the Fawbush-Miller and the Anthes methods with Foster's method indicating severe potential. The closest convective gust report available at the time of this investigation was at Alexandria, LA with 52 kts. This wind report, however, does not meet the proximity criteria and therefore cannot be used as verification for these estimated wind gusts.

Surface temperatures that afternoon reached  $72^{\circ}\text{F}$  at Jackson with many stations south of Vicksburg reaching the mid 70's and low 80's just before convective activity began in the area (Fig. 19). While there is not a reporting station at Vicksburg, it is likely the temperature in and around the Vicksburg vicinity reached the mid 70's. Figure 20 displays the actual 0000 UTC 21 February sounding from the Jackson launch site. The sounding analysis, Table 11, is also included. Note the Lifted Index for the actual evening sounding,  $-3.8$ ,

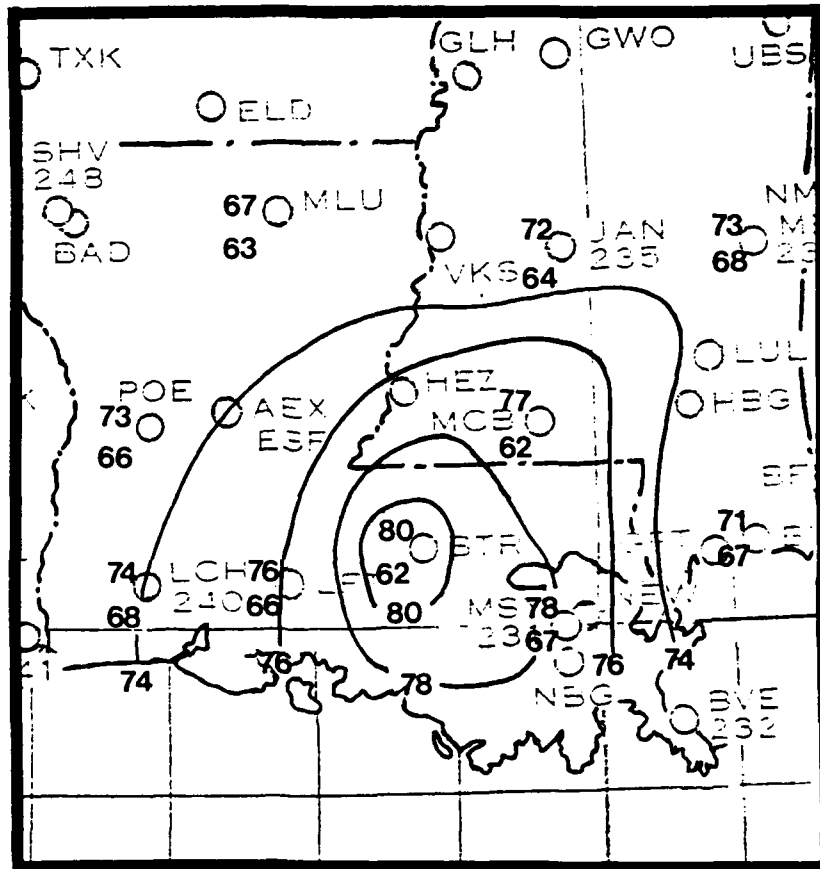


Fig. 19 Surface temperatures and dewpoint temperatures for Louisiana and Mississippi stations at 2100 UTC 20 February 1989.

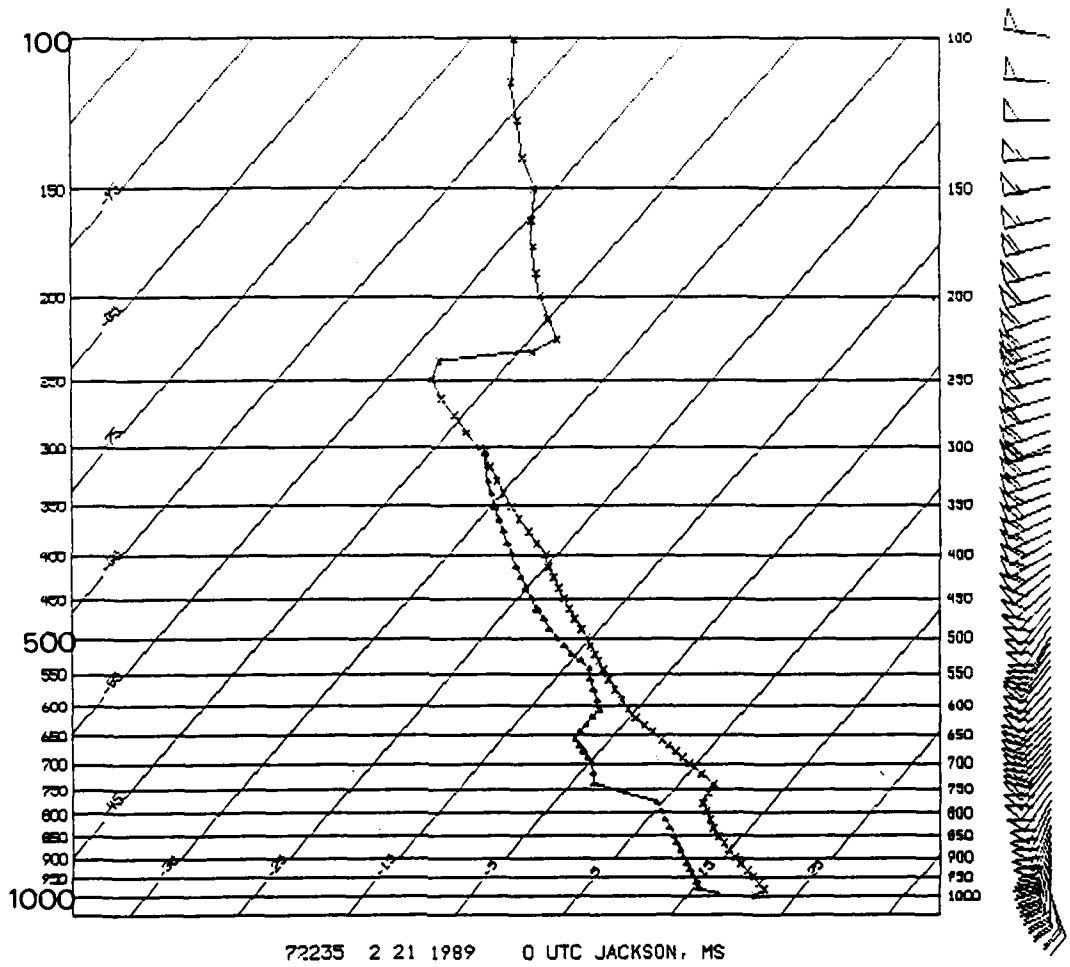


Fig. 20 Upper air sounding for Jackson, MS at 0000 UTC 21 February 1989.



agreed well with the forecast sounding's LI of -4.4 as computed from the forecast sounding which included geostrophic thermal advection. Also note that a small inversion was produced by the forecast sounding in Fig. 18 just above 850 mb and the actual sounding in Fig. 20 indicated an isothermal layer just above 800 mb. These two features are interesting.

## 5. CONCLUSIONS

### 5.1 SUMMARY

This research has developed a sounding analysis package featuring diagnostic/prognostic algorithms for the improvement of severe convective weather forecasting. Specifically, more accurate hail and convectively-driven wind gust forecast methods are proposed as alternatives to those currently used by the USAF Air Weather Service. The research demonstrated the operational utility of these methods as applied to an interactively-derived forecast sounding.

Automated methods for estimating hailstone size and convectively-driven wind gusts were developed and validated against techniques used by the USAF Air Weather Service. Validation results using proximity soundings for 58 severe hail events and 47 severe wind events selected from AVE-SESAME I and II, OK PRE-STORM, and July-August 1986 demonstrate increased accuracy by the proposed methods. Specifically, those results for the 58 hail events are:

Pino-MooreAWS TR-200

Correlation coefficient:

= 0.50

0.19

Student-t statistic significant at the:

0.5% level

10% level

Validation of the Fawbush and Miller (1953) (scatter = 20.5), Foster (1958) (scatter = 26.3), and Anthes (1977) (scatter = 9.8) wind methods suggest Anthes' method to be more operationally useful.

An interactive forecast sounding algorithm considers diurnal changes to a 1200 UTC sounding expected to occur in lower tropospheric levels. Estimating surface heating from sunrise to the time of convection is computed by considering the fraction of the incident solar radiation available for sensible heating of the well-mixed layer. Modifying factors such as cloud cover, soil moisture, and low-level moisture are considered. Adjustment of the mean-mixing ratio is made by forecasting the afternoon surface dewpoint temperature from a local area surface chart. Changes to the middle and upper levels are estimated by taking a fraction of the mean geostrophic advection of temperature for consecutive layers and adjusting the 1200 UTC sounding accordingly.

Interactive capability allows for final adjustment of any or all of the data levels.

Validation using 15 severe hail events revealed significant improvement in operational forecasts for these events with a mean error of 0.03 cm in the estimated hailstone diameter. This mean error is compared to values of -2.16 cm and -1.18 cm for the 1200 UTC and proximity soundings, respectively. Two of the hail events were accompanied by severe convectively-driven wind gusts. While the morning soundings (1200 UTC) did not favor downdraft conditions for either case, winds estimated by Anthes' method for one of the forecast soundings reached severe threshold (greater than 55 kts) while the other forecast sounding indicated near severe threshold potential (43 kts).

To further illustrate the operational utility of the proposed forecast sounding, a case study of a severe storm episode from 20 February 1989 is presented. The forecast sounding was completed for a proximity sounding from Jackson, MS at 1200 UTC 20 February. A hail diameter estimate of 5.19 cm was obtained from the Pino-Moore hail algorithm based on the forecast sounding. The hail event at Vicksburg,

MS verified hailstones with diameters up to 5.08 cm.

## 5.2 FUTURE CONSIDERATIONS

The hail and wind events used in the validation of the proposed methods were of severe levels (hail greater than or equal to 1.91 cm and winds greater than 55 kts). It is recommended that the hail and wind algorithms be tested for non-severe events. It was earlier proposed in section 4.1.1 that for small hail events (less than 1 cm), the algorithm would allow a value 0.87 for the drag coefficient. Also mentioned earlier in section 4.2 was a proposal of including the effects of water loading above the LFS in the Anthes' wind gust algorithm. The impact of these two modifications to the hail/wind algorithms could be assessed during an operational test of the Pino-Moore sounding analysis package.

In formulating the algorithm for the forecast sounding, atmospheric processes which contribute to the changes of the middle and upper level lapse rates were either neglected or simplified. The complete role of the geostrophic advection of temperature in the evolutionary changes of the atmospheric thermodynamic structure is not

completely understood. This alone could compromise a lengthy study. Could the modification factors used by the algorithm be fined tuned? What other atmospheric processes, such as low level thermal advection can be represented by the algorithm? These are just a few considerations that could be addressed by future research.

## APPENDIX A

Many of the thermodynamic parameters calculated by the sounding analysis program require thermal and moisture information characteristic of the surface layer (lowest 100 mb layer of the sounding). The average potential temperature ( $T_{\text{bar}}$ ) and the average mixing ratio ( $w_{\text{bar}}$ ) of this layer are computed by taking the average potential temperature a little layer at a time and multiplying that temperature by the fraction that layer is of 100 mb. The average mixing ratio is computed similarly but weighted according to  $p^k$ .

$$\text{K Index} = T_{850} + T_{d850} - T_{500} - DD_{700}$$

$$\text{Total-totals Index} = T_{850} + T_{d850} - 2T_{500}$$

SWEAT Index - Standard method after AWS TR-79/006

Showalter Index - Lifts a parcel dry adiabatically from 850 mb to its LCL and then moist adiabatically to 500 mb

$$SI = T_{\text{parcel}} - T_{500}$$

**Lifted Index** - Lifts the surface parcel defined by the average potential temperature and average mixing ratio of the lowest 100 mb moist adiabatically to 500 mb.

$$LI = T_{\text{parcel}} - T_{500}$$

**SELS Lifted Index** - Computes the LI using the SELS method but only for the 1200 UTC sounding. The method adds 2°C to the mean potential temperature of the lowest 100 mb. The LI is then computed as described above.

**Max Temperature Based on SELS LI** - Computes the maximum surface temperature using the value of the mean potential temperature + 2°C used in the SELS LI. The algorithm lowers a parcel dry adiabatically to the surface.

**Best Lifted Index** - First computes the maximum saturated wet bulb potential temperature ( $\theta(w_{\text{max}})$ ) of the surface layer using 50 mb layers starting at the surface to surface-50 mb and incrementing the lower boundary every 10 mb going no higher than 100 mb above the surface. The algorithm then lifts  $\theta(w_{\text{max}})$  moist adiabatically to 500 mb.

Best Lifted Index = most unstable value of

$$T_{\text{parcel}} - T_{500}$$

LID Strength Index - Computed as  $\theta(\text{swl}) - \theta(\text{wmax})$ , where  $\theta(\text{swl})$  is the maximum wet bulb potential temperature between the surface and 500 mb.

Lifted Condensation Level - Using the values of the mean potential temperature and mixing ratio of the lowest 100 mb, the parcel is lifted dry adiabatically to the LCL.

Convective Condensation Level - Using the mixing ratio corresponding to the surface dewpoint temperature, the algorithm finds the intersection of the mixing ratio line and the dry-bulb sounding. In certain cases, an inversion may exist above this intersection in which multiple CCLs exist. If more than one CCL exists, the algorithm displays the levels allowing the user to interactively choose the CCL. This CCL is then used in subsequent algorithms including calculating the convective temperature.

Convective Temperature Based on the CCL - Lowers a parcel dry adiabatically from its CCL to the

surface.

**Level of Free Convection** - The LFC is found by lifting a parcel using the boundary layer LCL moist adiabatically to where it intersects the dry-bulb curve. In some cases, the sounding may intersect the dry-bulb sounding more than once. If a second intersection is found, the algorithm displays the levels allowing the user to interactively choose the LFC. This LFC is then used in subsequent algorithms.

**Equilibrium Levels (EL)** - After determining the positive area (either CCL or LFC based), the algorithm searches for the top of the positive area where the dry-bulb curve and the moist adiabat through either the CCL or LFC intersect. See Fig. 5.

**Positive Area (CCL based)** - Using the value of the CCL, a moist adiabat is constructed upward to the EL. The area bounded by this moist adiabat and the dry-bulb curve is the positive area.

**Negative Area (CCL Based)** - A dry adiabat is constructed downward from the CCL to the surface.

The area bounded by the dry-adiabat and the dry-bulb curve is the negative area.

**Convective Available Potential Energy (CAPE)** - A moist adiabat is constructed upward from the LFC to the EL. The area bounded by the moist adiabat and the dry-bulb curve is the CAPE.

**Convective Inhibition** - The negative area bounded on the right by the dry-bulb curve, at the bottom by the surface level, and on the left by the dry adiabat from the surface temperature to the LCL and by the moist adiabat from the LCL to the LFC.

**Vertical Wind Shear** - To compute the shear term, the algorithm sums up the density weighted  $u$  and  $v$  components for each level from the surface to 500 m above the surface and from the surface to 6000 m above the surface. The shear is then equal to the difference of the resultant wind vectors divided by the vertical distance of 5500 m.

**Bulk Richardson Number** - Computed by dividing the CAPE by the square root of the vertical wind shear.

**Precipitable Water** - Computes the mean pressures and

dewpoint temperatures for consecutive layers and then calculates the corresponding mixing ratio for each layer. The average mixing ratios for each layer are summed up and the precipitable water is calculated following a procedure from the NWS Forecasting Handbook, July 1979.

Height of the Wet-Bulb Zero - Determines the height where the wet-bulb temperature is  $0^{\circ}\text{C}$ .

W Max Based on the LFC - Using a boot strap method, the vertical velocity is calculated by lifting a parcel upward moist adiabatically from its LFC to its EL. The algorithm computes the temperature of the cloud,  $T_c$ , represented by this moist adiabat using (10). Using (11), the value of  $w$  is computed by integrating upward to the level where the parcel temperature is  $-10^{\circ}\text{C}$ .

W Max Based on the CCL - Follows the same procedures for the  $w$  max based on the LFC but uses the moist adiabat through the CCL.

Diameter of Hail Based on the LFC - Substitutes the value of  $w$  max based on the LFC approach into (5). Applies the melting algorithm described in section

## 3.1.3.

Diameter of Hail Based on the CCL - Follows the same procedures for the diameter of hail based on the LFC but uses the value of  $w_{max}$  based on the CCL. Also applies the melting algorithm from section 3.1.3.

Diameter of Hail Based on AWS TR-200 - Follows the procedures described in section 2.1, paragraphs 1 and 2.

Surface Wind Gusts Based on Fawbush-Miller - Follows the procedures described in section 2.2, paragraph 1.

Surface Wind Gusts Based on Foster - Follows the procedures described in section 2.2, paragraph 2.

Surface Wind Gusts Based on Anthes - Follows the procedures described in section 3.2.

## REFERENCES

- Air Weather Service (MAC), 1987 (Rev): The Use of the Skew-T, log-P Diagram in Analysis and Forecasting, AWS/TR-79/006, 144 pp.
- Anthes, R. A., 1977: A cumulus parameterization scheme utilizing a one-dimensional cloud model. Mon. Wea. Rev., 105, 270-286.
- Bilham, E. G., and E. F. Relf, 1937: The dynamics of large hailstones. Quart. J. R. Meteor. Soc., 63, 149-160.
- Bluestein, H. B., E. W. Mckaul, G. P. Byrd, and G. R. Woodall, 1988: Mobile sounding observations of a tornadic storm near the dryline: the Canadian, Texas, storm of 7 May 1986. Mon. Wea. Rev., 116, 1790-1804.
- Crum, T. D., and J. J. Cahir, 1983: Experiments in shower-top forecasting using an interactive one-dimensional cloud model. Mon. Wea. Rev., 111, 829-835.
- Doswell, C. A., 1985: The Operational Meteorology of Convective Weather Volume II: Storm Scale Analysis, NOAA Technical Memorandum ERL ESG-15, Environmental Sciences Group, 240 pp.
- \_\_\_\_\_, J. T. Schaefer, D. W. McCann, T. W. Schlatter, and H. B. Wobus, 1982: Thermodynamic analysis procedures at the National Severe Storms Forecast Center. Preprints, 9th Conf. on Weather Forecasting and Analysis, Amer. Meteor. Soc., Seattle, WA, 304-309.
- Fawbush, E. J., and R. C. Miller, 1953: A method for forecasting hailstone size at the Earth's surface. Bull. of the Amer. Meteor. Soc., 34, 235-244.
- \_\_\_\_\_, 1954: A basis for forecasting peak wind gusts in non-frontal thunderstorms. Bull. of the Amer. Meteor. Soc., 35, 14-19.
- Foster, D. S., 1958: Thunderstorm gusts compared with computed downdraft speed. Mon. Wea. Rev., 86, 91-94.

- \_\_\_\_\_, and F. C. Bates, 1956: A hail size forecasting technique. Bull. of the Amer. Meteor. Soc., 35, 135-140.
- Gesser, F., and D. Wallace, 1985: The Forecast Sounding. Air Weather Service (MAC), United States Air Force, 13 pp.
- Graziano, T. M., and T. N. Carlson, 1987: A statistical evaluation of lid strength on deep convection. Weather and Forecasting, 2, 127-139.
- Haltiner, G. J., and R. T. Williams, 1980: Numerical Prediction and Dynamic Meteorology, John Wiley and Sons, 477 pp.
- Leftwich, P. W., 1984: Operational experiments in prediction of maximum expected hailstone diameter. Preprints, 10th Con. on Weather Forecasting and Analysis, Amer. Meteor. Soc., Clearwater Beach, FL, 525-528.
- \_\_\_\_\_, 1986: Operational estimations of hail diameter from VAS-derived vertical sounding data. Preprints, 2nd Conf. on Satellite Meteorology/Remote Sensing and Applications, Amer. Meteor. Soc., Williamsburg, VA, 193-196.
- Macklin, W. C., 1963: Heat transfer from hailstones. Quart. J. Royal. Meteor. Soc., 89, 360-369.
- \_\_\_\_\_, 1964: Factors affecting the heat transfer from hailstones. Quart. J. Royal. Meteor. Soc., 90, 84-90.
- Maddox, R. A., 1973: A Study of Tornado Proximity Data and an Observationally Derived Model of Tornado Genesis. Atmos. Sci. Paper #212, Dept. of Atmos Sci., Colo. State Univ., Fort Collins, Colo, 101p.
- Mason, B. J., 1956: On the melting of hailstones. Quart. J. Royal. Meteor. Soc., 82, 209-216.
- Matson, R. J., and A. W. Huggins, 1980: The direct measurement of the sizes, shapes and kinematics of falling hailstones. J. Atmos. Sci., 37, 1107-1125.
- McGinley, J., 1986: Mesoscale Meteorology and Forecasting. Amer. Meteor. Soc., Boston, MA, 657-688.

- Miller, R. C., 1972: Notes on Analysis and Severe-Storm Forecasting Procedures of the Air Force Global Weather Central. Air Weather Service (MAC), United States Air Force.
- Prosser, N. E., and D. S. Foster, 1966: Upper air sounding analysis by use of an electronic Computer. J. Appl. Meteor., 5, 296-300.
- Schaefer, J. T., 1975: Moisture stratification in the "well-mixed" boundary layer. Preprints, 9th Conf. Severe Local Storms, Amer. Meteor. Soc., Norman, OK, 45-50.
- Sellers, W. D., 1965: Physical Climatology. University of Chicago Press, 272 pp.
- Storm Data, 1986: National Oceanic Atmospheric Administration Environmental Data Series, Asheville, N.C., 28, #8, 58 pp.
- \_\_\_\_\_, 1986: National Oceanic Atmospheric Administration Environmental Data Series, Asheville, N.C., 28, #7, 78 pp.
- \_\_\_\_\_, 1985: National Oceanic Atmospheric Administration Environmental Data Series, Asheville, N.C., 27, #6, 46 pp.
- \_\_\_\_\_, 1985: National Oceanic Atmospheric Administration Environmental Data Series, Asheville, N.C., 27, #5, 66 pp.
- \_\_\_\_\_, 1979: National Oceanic Atmospheric Administration Environmental Data Series, Asheville, N.C., 21, #5, 32 pp.
- \_\_\_\_\_, 1979: National Oceanic Atmospheric Administration Environmental Data Series, Asheville, N.C., 21, #4, 21 pp.

## Biography of the Author

John Philip Pino [REDACTED]

[REDACTED] and lived in Attleboro, Massachusetts. His interest in meteorology developed while attending Attleboro High School where he was a member of the weather observation station for four years. Upon graduation, he was awarded the Bausch & Lomb Honorary Science Award.

He pursued his interest in meteorology at The Pennsylvania State University sponsored by an Air Force ROTC scholarship. Along with receiving a Bachelor of Sciences degree in meteorology, he was commissioned a second lieutenant in the United States Air Force upon graduation.

Before attending Saint Louis University, he served as Wing Weather Officer to the 436<sup>th</sup> Military Airlift Squadron at Dover AFB, DE from 14 October 83 to 13 January 1986. Assigned as Assistant Chief Forecasting Services Division, Headquarters Air Weather Service from 15 January 1986 until 15 August 1987, he published 9 Air Weather Service Forecaster Memos on severe weather forecasting.